Recommendations on the most reliable predictor variables and evaluation of inter-relationships (D 13)

Part II- Evaluation of predictors specific to method and region

András Bárdossy and Yeshewatesfa Hundecha
University of Stuttgart

Introduction

The purpose of this work is to evaluate the GCM simulated variables that are potentially used for the downscaling of extreme precipitation and temperature within the Rhine basin by comparing them with the corresponding NCEP reanalysis variables. Based on the results obtained from this work and subsequent evaluation of the predictor predictand relationship, recommendations on the most reliable predictor variables will be made. The potential predictor variables were selected in previous works (D10) and applied in downscaling extreme precipitation and temperature indices (D12).

Data sets and methodology

A set of derived potential predictor variables are used in the downscaling model utilized for the downscaling of extreme precipitation and temperature within the case study region. These include:

- Eastward moisture flux at 700hPa pressure level
- Vorticity and divergence of the wind fields at 500, 700, and 850hPa pressure levels
- Objective circulation patterns derived from sea level pressure

For the computation of these predictor variables, the x and y components of the wind speed at 500, 700, and 850hPa levels; the specific humidity at 700hPa level and sea level pressure fields were used. These data sets were taken from the NCEP reanalysis data set and the the three ensembles of the HadAM3P control run on a 2.5° × 2.5° grid over a standard European window. The circulation patterns were derived using the fuzzy rule based classification technique from the NCEP sea level pressure and discharge data as explained in D10.

Evaluation of the predictors derived from the HadAM3P data against that of the NCEP data set was made on the seasonal basis. In the downscaling model, seasonal measures of extreme of the predictor variables are used. These are the seasonal 10^{th} and 90^{th} percentile values of the predictor variables. The evaluation was therefore made on the seasonal mean values as well as these measures of extreme. The seasonal mean values and extreme measures, as well as the standard deviations of the daily values and the seasonal extreme measures of the HadAM3P predictors were calculating by considering all the three ensembles as a single 90-year series. The corresponding values of the NCEP predictors were calculated ove the year 1961 to 1990. The biases of the HadAM3P based seasonal mean values and the mean of the yearly seasonal extreme measures against that of the NCEP based values were computed and mapped over the entire region of study. Similarly, the ratio of the standard deviations of the daily values of the predictor variables in each season and the yearly seasonal 10^{th} and 90^{th} percentile values were computed and mapped.

The above evaluation procedure was applied to predictors that have numerical values. For the circulation patterns, the evaluation was made by comparing the seasonal frequency and persistence of the circulation patterns associated with extreme precipitation.

Summary of Results

Maps of the biases of the seasonal mean and extreme measures as well as the ratios of the standard deviations of the daily values and the yearly seasonal extreme values for each predictor are shown in the appendix. Following is a brief discussion of the observations on the evaluation.

Moisture flux

The bias of the seasonal mean moisture flux shows spatial variability, which is variable seasonally. In winter, the HadAM3P moisture flux is a bit over estimated over the British isles and the bias decreases in all directions. In most parts of central Europe, the bias is close to zero and becomes negative further to the north and the south. In spring, the spatial variability of the bias is less and the HadAM3P moisture flux seems to be a bit underestimated in most parts of Europe compared to that of the NCEP. A similar situation is noticed in autumn except that the underestimation gets stronger towards the east and south Western Europe. In summer, the HadAM3P moisture flux is a bit under estimated in the central and southern parts of Europe. A little overestimation is noticed in some parts of the north.

Comparison of the variability of the flux at a given location as measured by the ratio of the standard deviations of the daily values shows that the HadAM3P moisture flux shows slightly higher variability in the central part of Europe and slightly lower variability in the northern and southern parts in the winter season. In spring, in most parts of Western Europe the variability of the HadAM3P and the NCEP fluxes show similar variability. In summer, the HadAM3P flux is a bit less variable than that of the NCEP in most parts of the region. In autumn, the degree of variability is more or less similar for both the HadAM3P and the NCEP fluxes and the variability shows spatial uniformity. Generally, the difference in variability is not that much in all seasons as the ratio of the standard deviations remains between 0.8 and 1.2 in most parts of Europe.

The bias of the lower extreme of the moisture flux as measured by the 10th percentile seasonal value shows a similar seasonal pattern like the bias of the mean seasonal values. The difference in the variability of the values, however, is noticed to be strong in some areas. In winter, the ratio of the standard deviations between the HadAM3P and the NCEP 10th percentile fluxes shows values around 1 in most parts of the central part of Europe. But the value goes lower towards the north and the south. In spring and autumn, the ratio decreases from around 1.0 in the central part of Europe to a much lower value towards the east. In summer, the HadAM3P moisture flux shows higher variability in the Mediterranean area and some parts of the Scandinavia, while it shows less variability in the other parts.

The bias of the upper extreme, i.e., the 90th percentile seasonal flux also shows similar seasonal patters. But the magnitudes of the biases are higher. Comparison of the variability of the 90th percentile HadAM3P and NCEP moisture fluxes shows that in spring and autumn, they show more or less similar variability in most parts of the region. In winter the HadAM3P moisture flux shows less variability in the northern Atlantic area and the Mediterranean area.

In summer it shows more variability in the southern Scandinavian area compared to that of the NCEP.

Vorticity

The bias between the seasonal mean HadAM3P and the NCEP vorticities displays more or less similar spatial pattern for all the three pressure levels. In winter it attains its maximum negative value over the southwestern part of Europe and increases gradually to a positive value in all directions. It increases faster in the northwest direction. While it remains negative in most of the southern part, it gets positive in the northern part of the region. A similar bias pattern is observed in spring, although less stronger. In summer, there is a slight positive bias in the central part of Europe and shifts to negative values towards the east and west directions and gets more positive towards the Mediterranean area. In autumn, the bias structure shifts from slightly negative bias over southwest Europe and northeast Europe to a slightly positive bias region in the central part.

The ratio of the standard deviations also displays similar pattern for all pressure levels. Both the HadAM3P and NCEP daily moisture fluxes show more or less similar variability, as the ratio of their standard deviations remains close to one.

The spatial structure of the bias of the extreme seasonal 10th and 90th percentile vorticities are similar to that of the seasonal mean vorticity. The ratio of the standard deviations, however, doesn’t show any defined spatial structure and varies over a wide range in all seasons.

Divergence

The bias of the mean seasonal divergence generally tends to be close to zero over the region for all seasons. There is no clear spatial structure on the bias. Pockets of slightly positive and negative bias are scattered all over the region.

The ratio of the standard deviation between the HadAM3P and NCEP daily values of divergence generally has a value greater than 1, which is very high over the alps, Iberia and Scandinavia. The pattern remains the same for all seasons but the magnitude of the ratio increases with the pressure level.

The bias of the 10th percentile extreme divergence is negative throughout the region, with the magnitude of the bias even getting larger over the Alps and the Scandinavia. The spatial pattern of the bias is similar for all seasons. The ratio of the standard deviation shows similar variability like the mean seasonal divergence.

The 90th percentile extreme seasonal divergence on the other hand shows a positive bias over most of the region in all seasons. The strongest bias is, like in the 10th percentile divergence, over the Alps, Iberia, and the Scandinavia. Areas of higher ratio of standard deviation remain similar to that of the mean seasonal and the 10th percentile seasonal divergence, their magnitude increasing with the pressure level.

Circulation Patterns

The NCEP sea level pressure fields were classified into twelve circulation patterns and three of them are associated with extreme precipitation (CP04, CP10, and CP11). The HadAM3P sea level pressure fields were also classified into similar patterns and the seasonal frequency and persistence of the CPs are compared with the corresponding CPs derived from the NCEP sea level pressure fields. Tables 1 to 3 show comparison of the mean seasonal frequency, mean persistence and mean maximum seasonal persistence of the HadAM3P and NCEP CPs

In general, except in summer, the wet CPs derived from the HadAM3P pressure field appear to be more frequent than the corresponding CPs derived from the NCEP pressure fields for all seasons. In summer, the opposite situation is noticed. Both the mean and the maximum seasonal persistence of the wet CPs tend to be a bit higher for HadAM3P pressure fields than the corresponding NCEP fields in all seasons.

Table 1: Mean seasonal frequency of CPs associated with extreme precipitation

CP type	Winter		Spring		Summer		Autumn	
	NCEP	HadAM3P	NCEP	HadAM3P	NCEP	HadAM3P	NCEP	HadAM3P
CP04	0.060	0.071	0.062	0.076	0.072	0.069	0.052	0.072
CP10	0.070	0.048	0.070	0.065	0.082	0.075	0.049	0.054
CP11	0.074	0.121	0.089	0.097	0.092	0.081	0.084	0.099
All wet CPs	0.204	0.240	0.221	0.237	0.245	0.226	0.185	0.225

Table 2: Mean seasonal persistence of CPs associated with extreme precipitation (days)

CP type	Winter		Spring		Summer		Autumn	
	NCEP	HadAM3P	NCEP	HadAM3P	NCEP	HadAM3P	NCEP	HadAM3P
CP04	1.47	1.50	1.32	1.48	1.32	1.40	1.41	1.49
CP10	1.48	1.40	1.61	1.61	1.51	1.73	1.27	1.48
CP11	1.61	1.77	1.66	1.53	1.37	1.37	1.57	1.63
All wet CPs	2.26	2.29	2.04	2.21	1.78	2.02	1.91	2.28

Table 3: Mean of the maximum seasonal persistence of CPs associated with extreme precipitation (days)

CP type	Winter		Spring		Summer		Autumn	
	NCEP	HadAM3P	NCEP	HadAM3P	NCEP	HadAM3P	NCEP	HadAM3P
CP04	2.20	2.40	2.10	2.39	2.10	2.23	1.94	2.49
CP10	2.60	2.01	2.55	2.44	2.55	2.81	1.77	2.27
CP11	2.83	3.34	2.81	2.71	2.39	2.27	2.87	2.98
All wet CPs	4.93	5.46	4.52	5.30	4.55	4.94	4.35	5.40

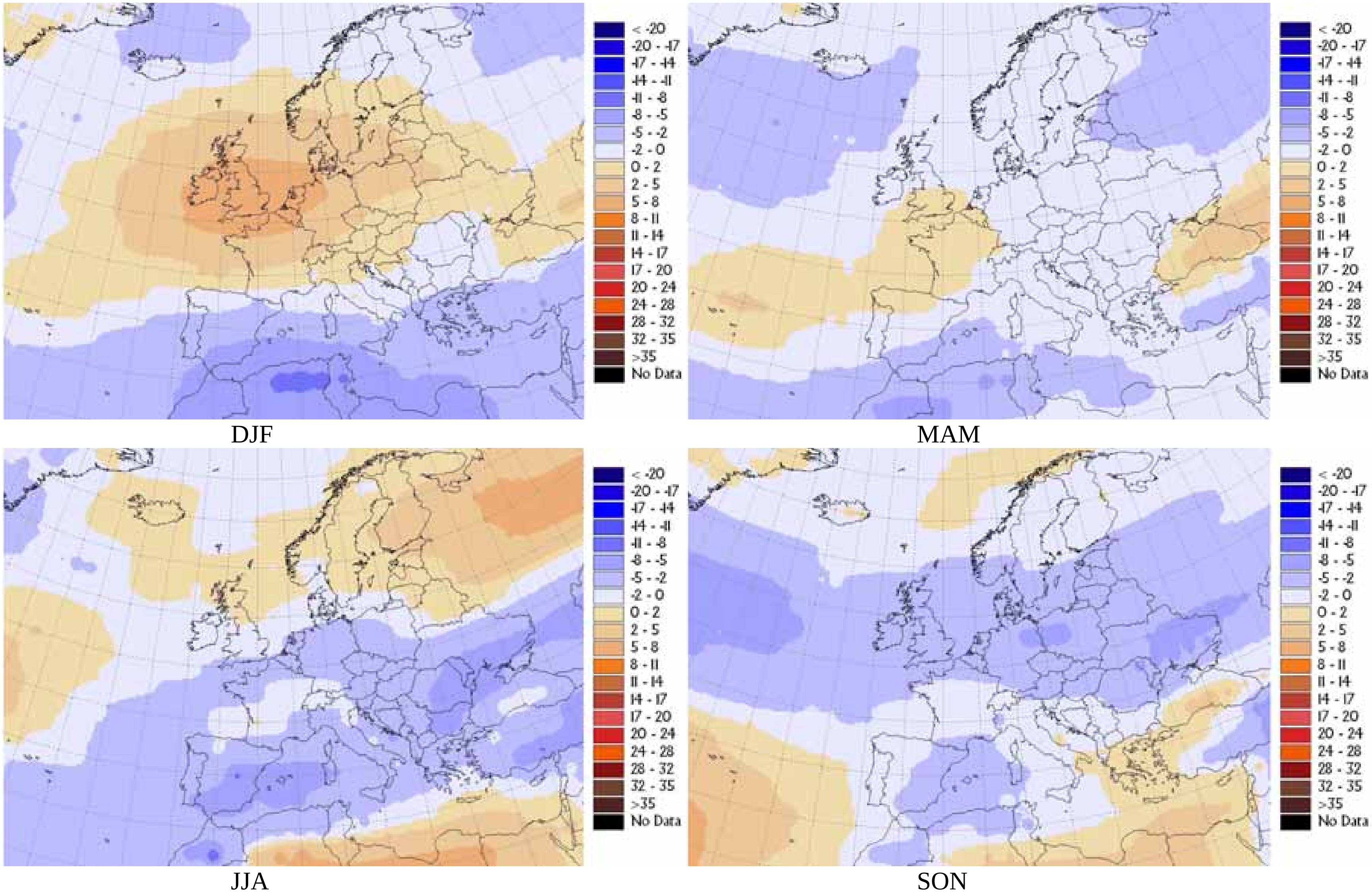

Bias of mean seasonal moisture flux at 700 hPa level (g.m/kg.s)

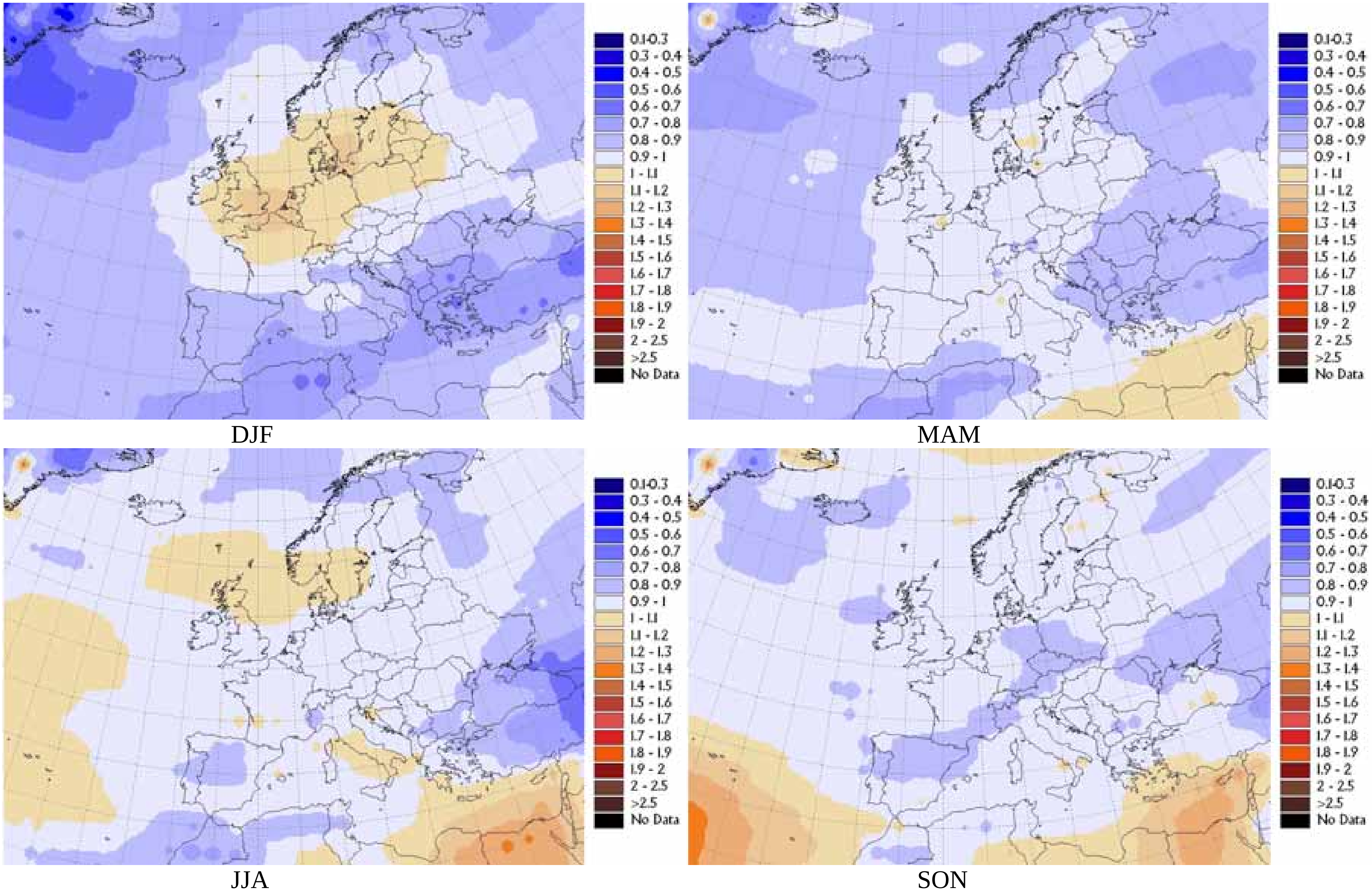

Ratio of standard deviations of daily values of moisture flux at 700 hPa level

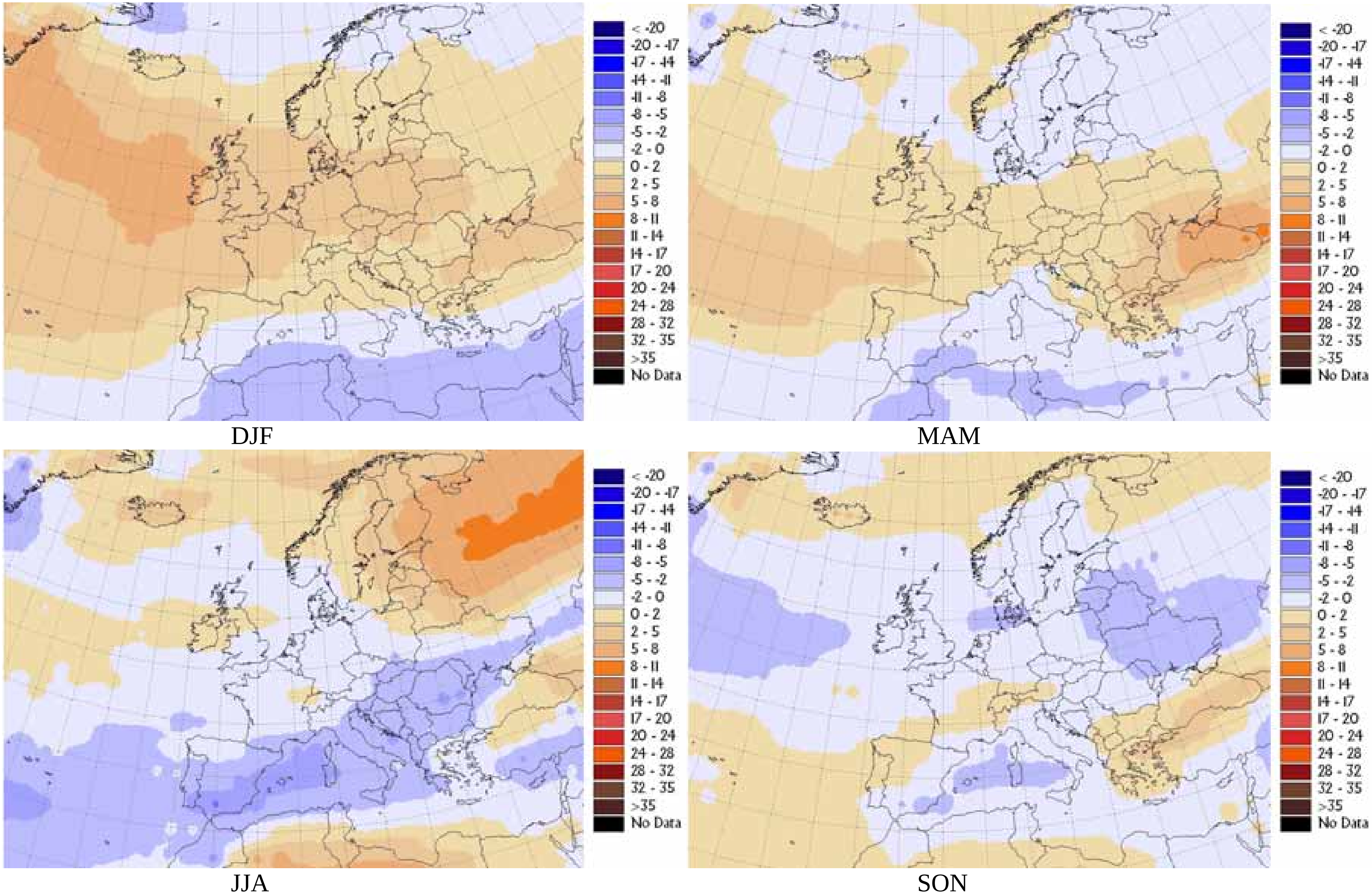

Bias of the average of the yearly 10th percentile seasonal moisture flux at 700 hPa (g.m/kg.s)

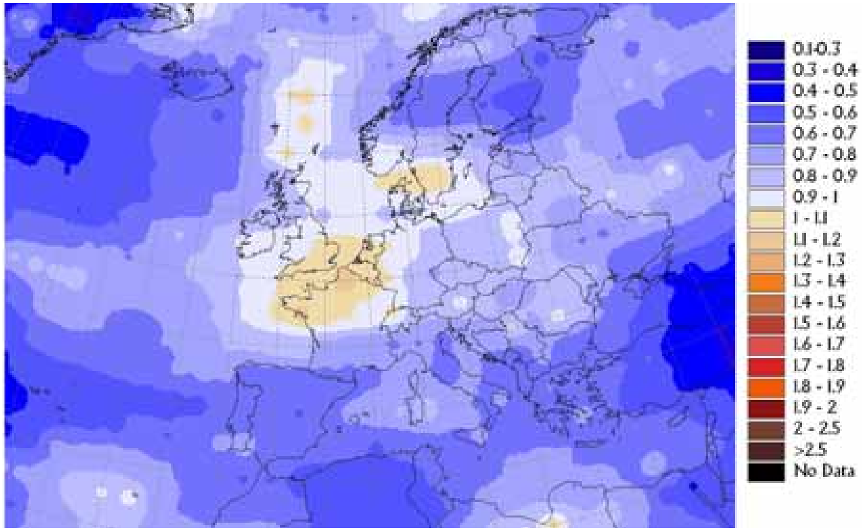

DJF

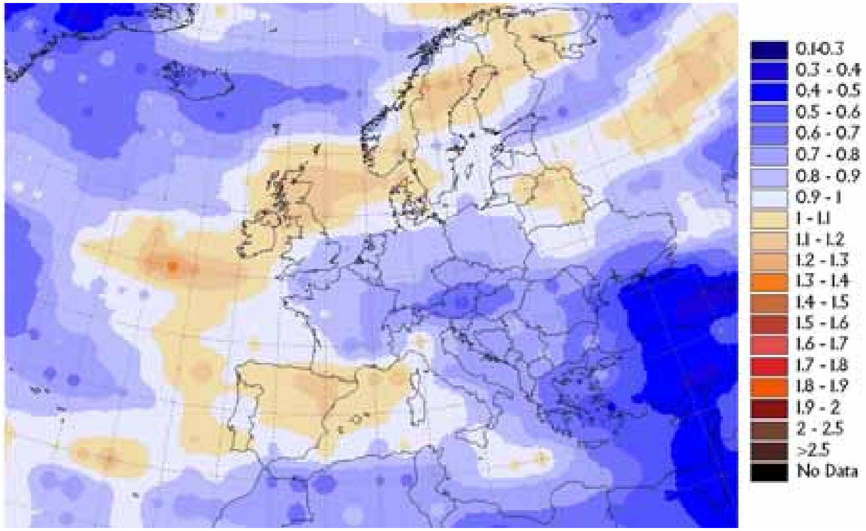

MAM

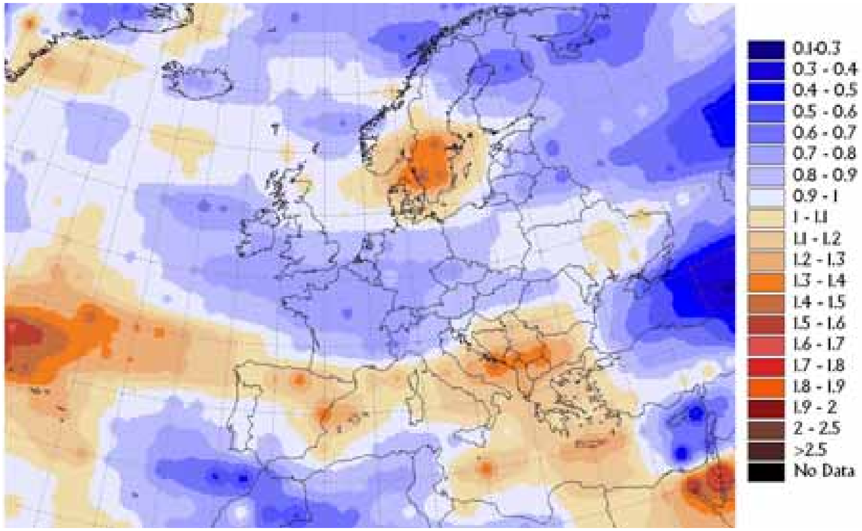

JJA

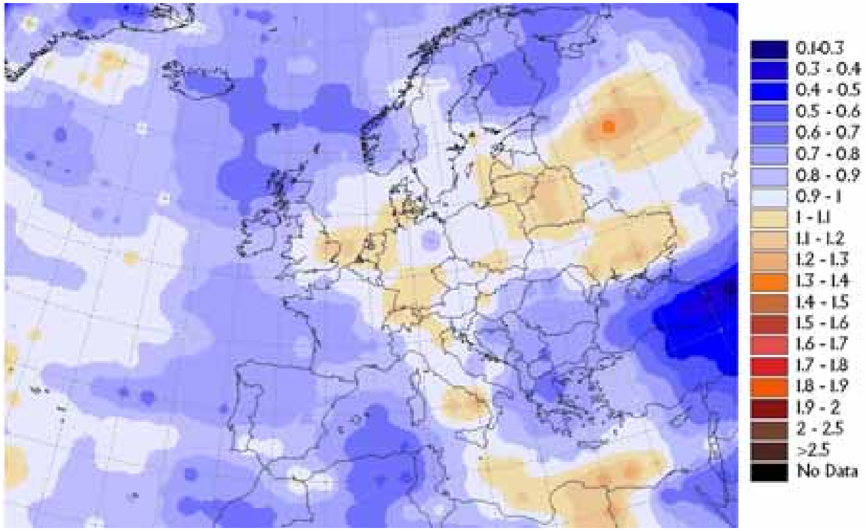

SON

Ratio of standard deviations of the yearly seasonal 10th percentile moisture flux at 700 hPa level

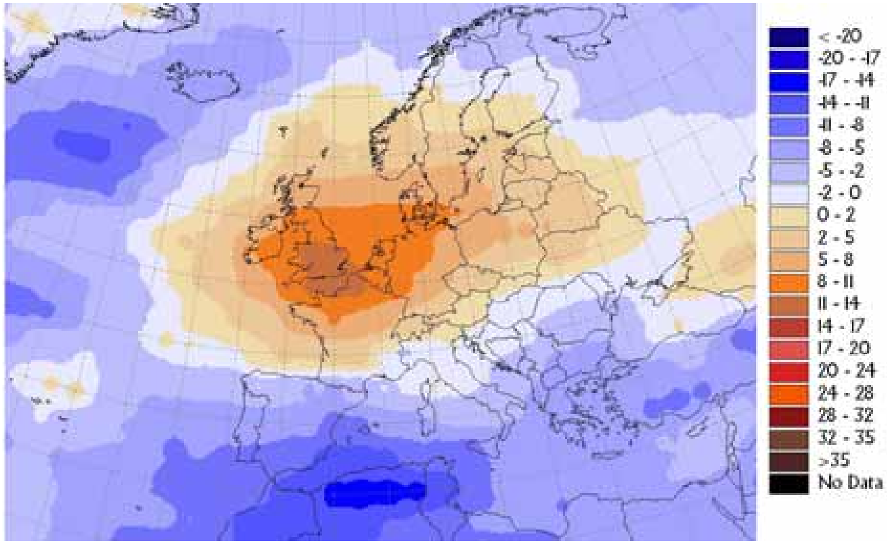

DJF

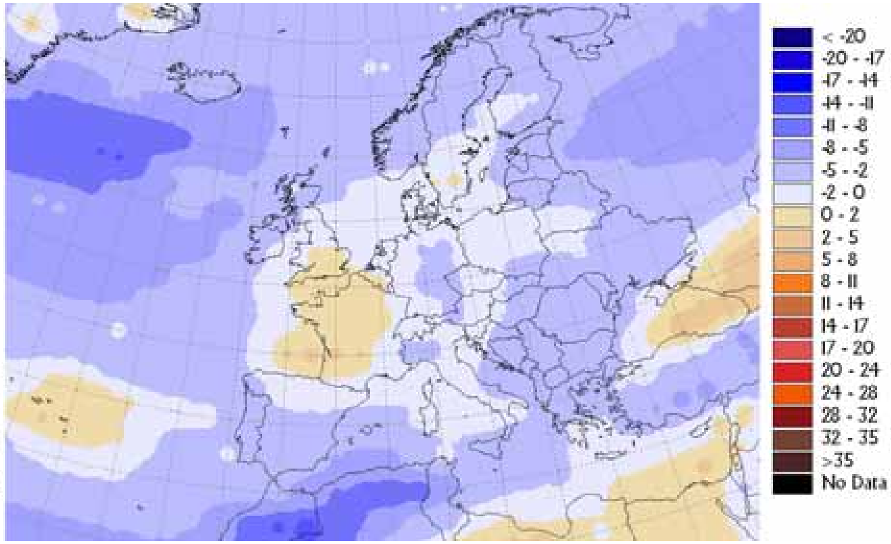

MAM

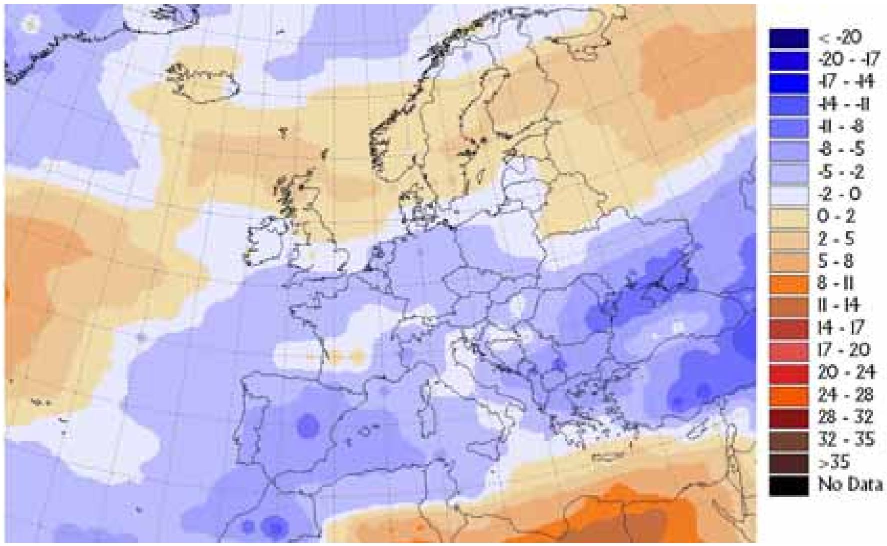

JJA

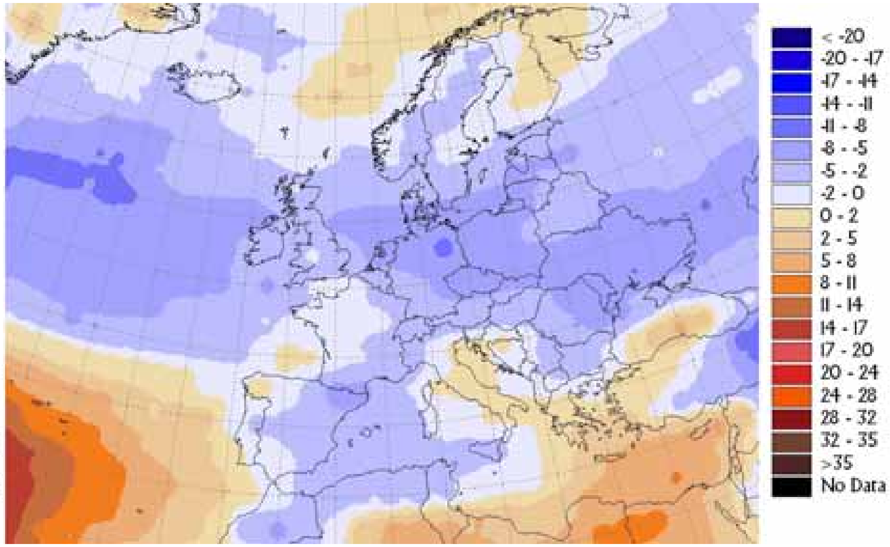

SON

Bias of the average of the yearly 90th percentile seasonal moisture flux at 700 hPa level (g.m/kg.s)

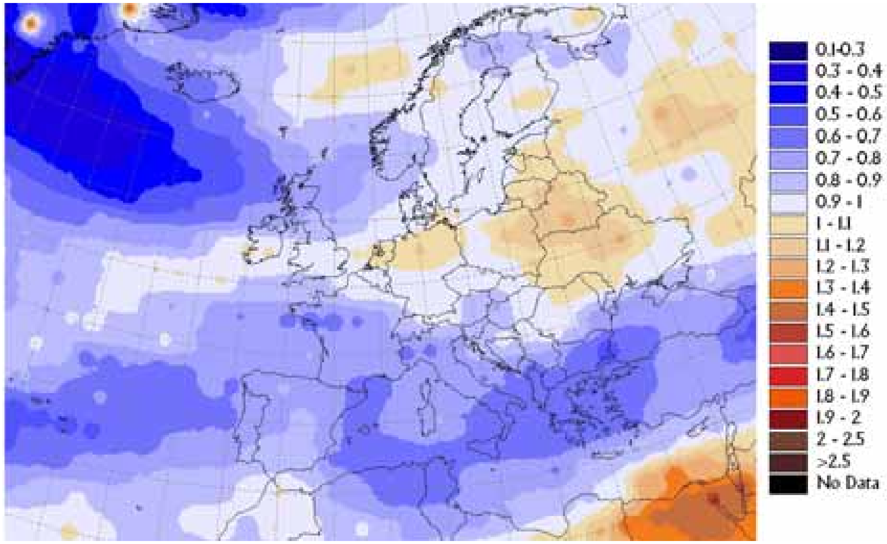

DJF

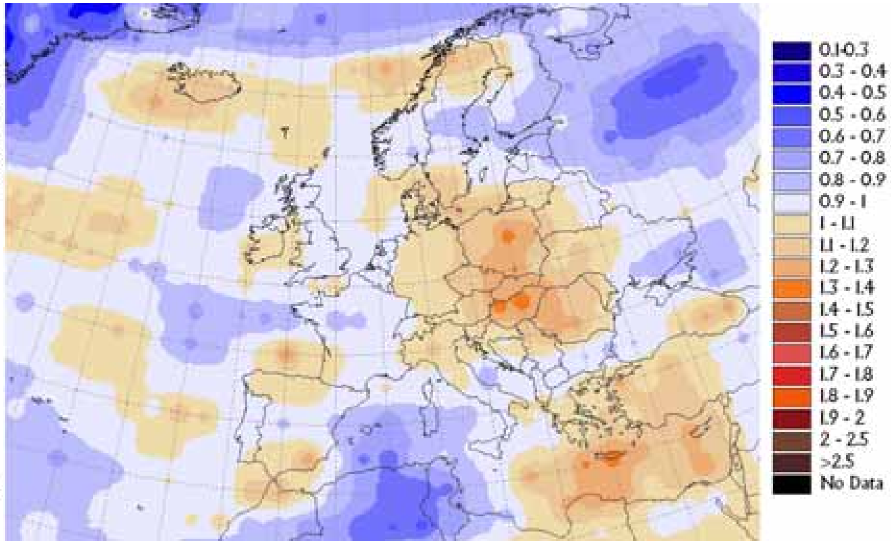

MAM

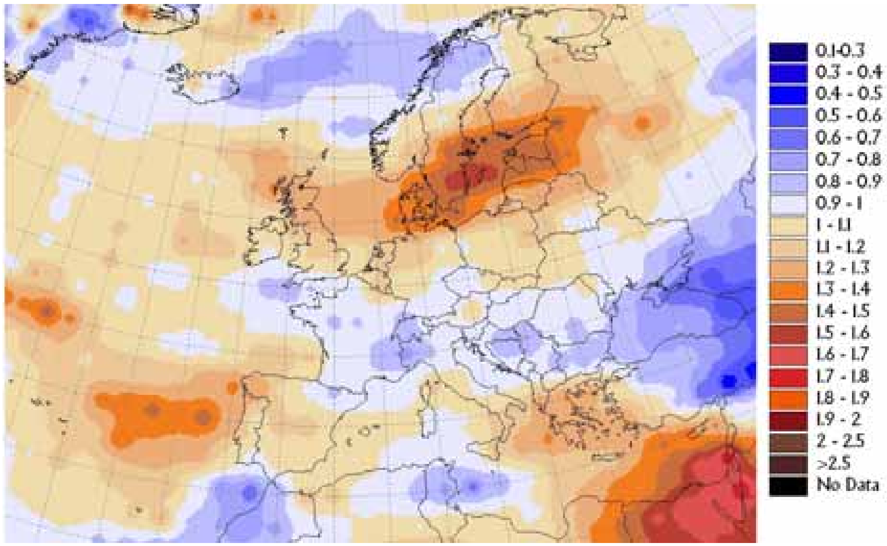

JJA

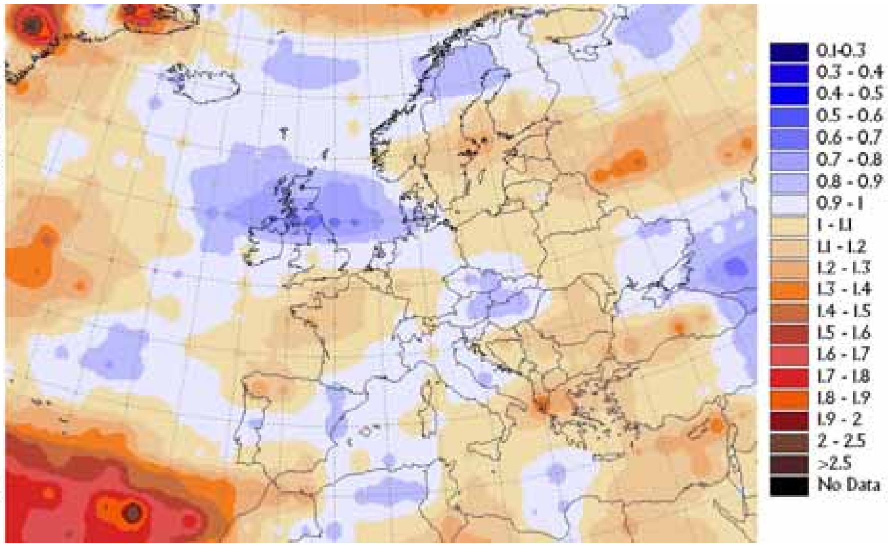

SON

Ratio of standard deviations of the yearly seasonal 90th percentile moisture flux at 700 hPa level

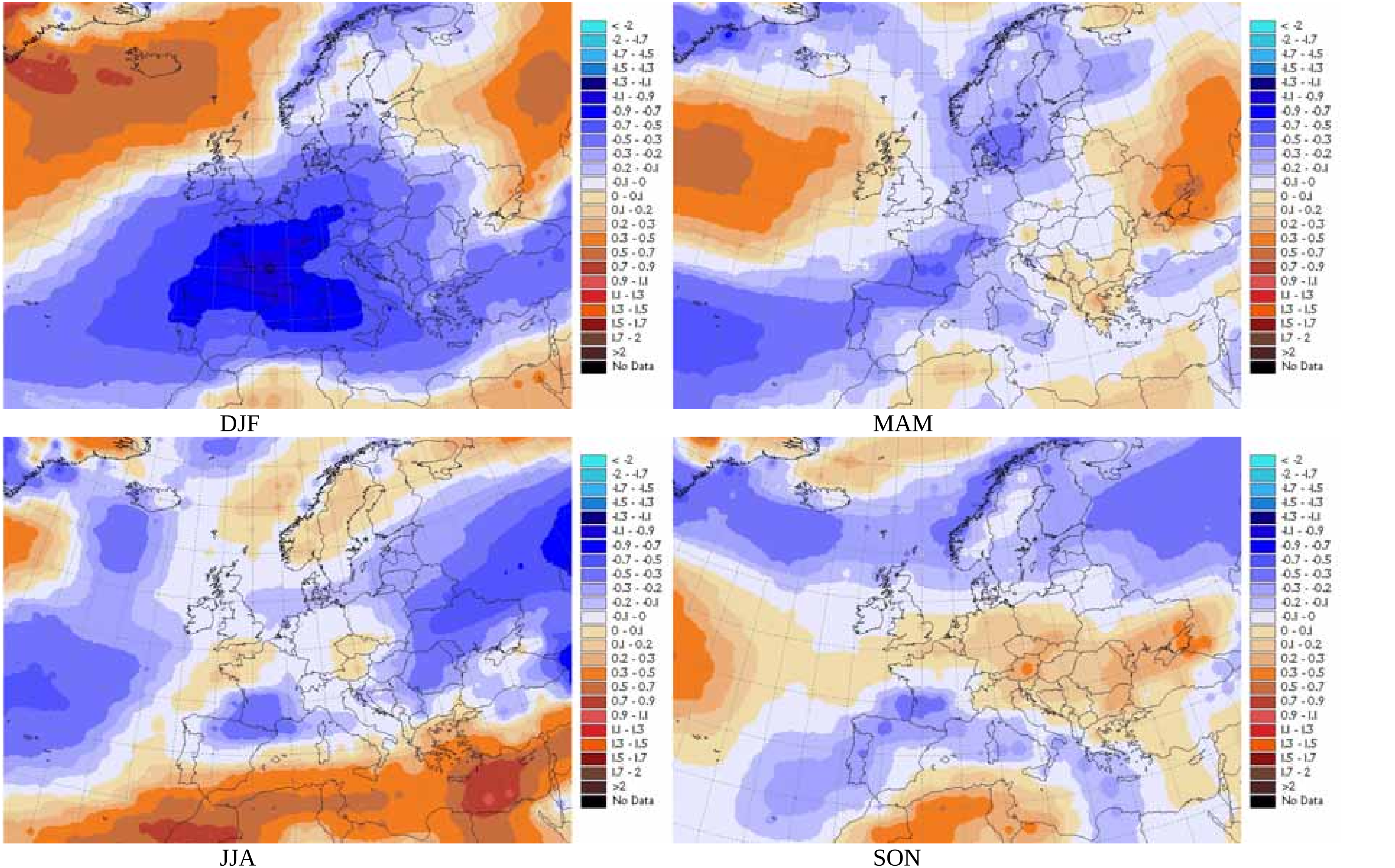

Bias of the seasonal mean vorticity at 500hPa level (10^{-5}/s)

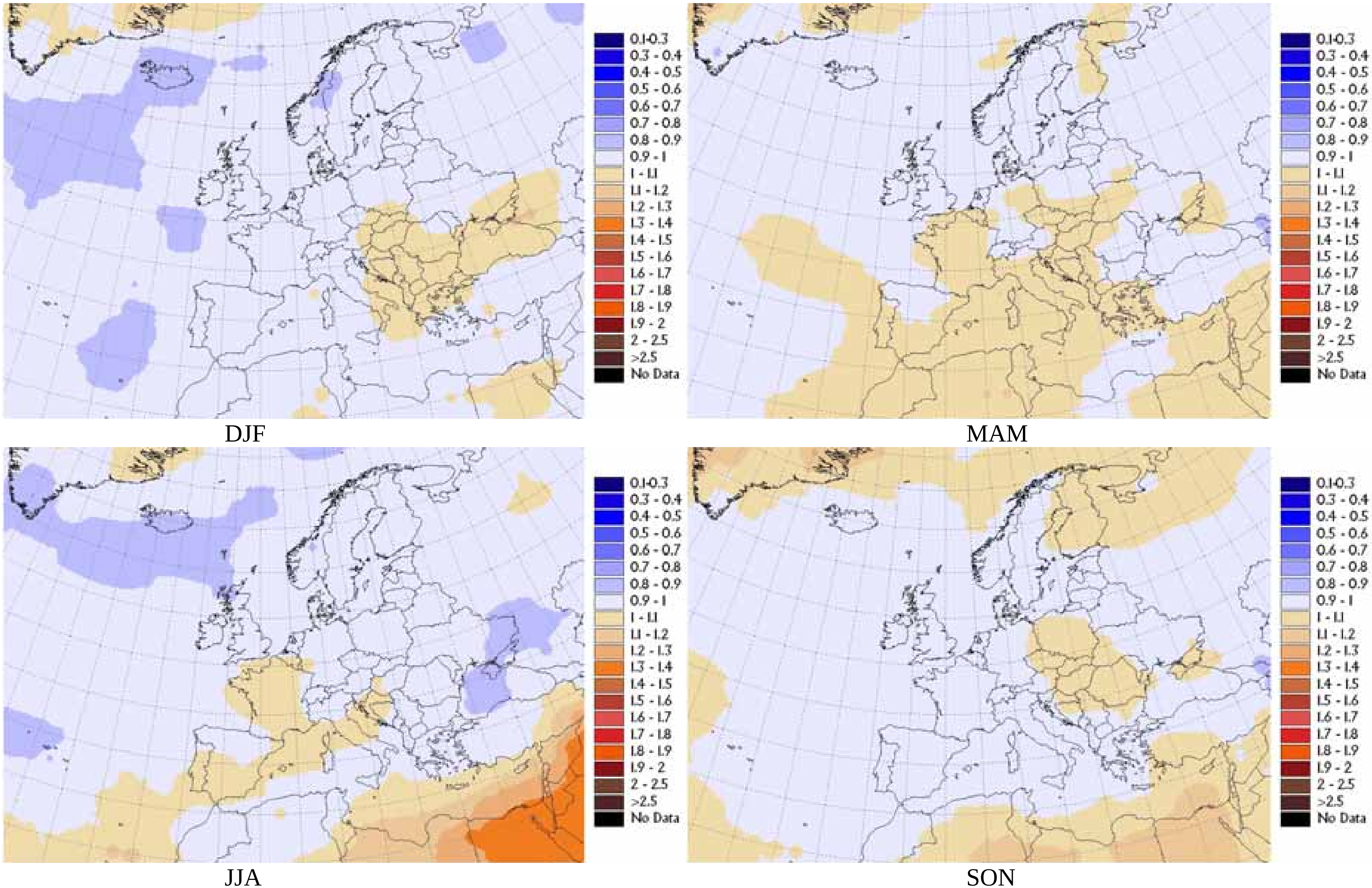

Ratio of standard deviations of daily values of vorticity at 500hPa level

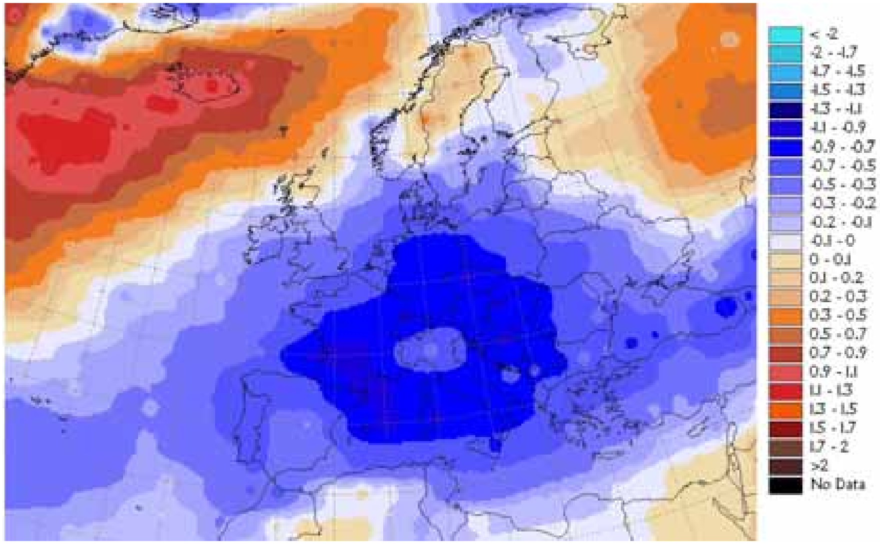

DJF

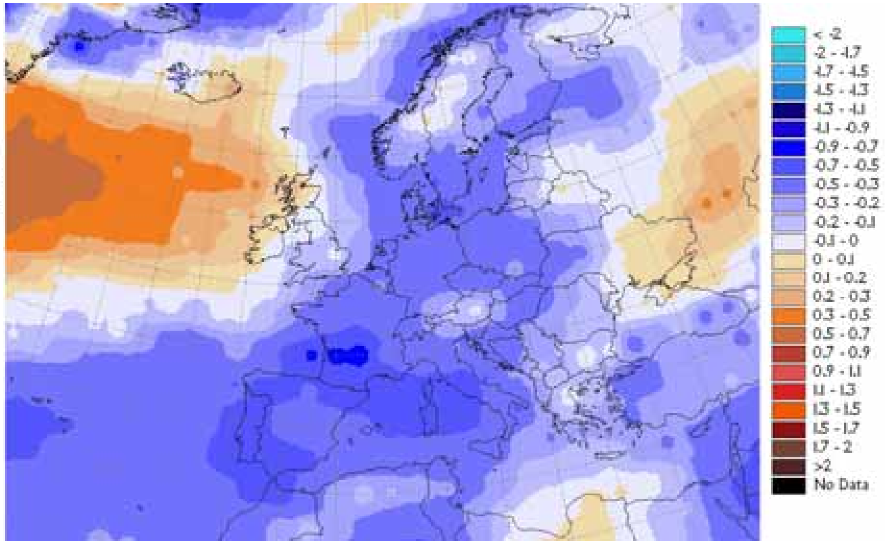

MAM

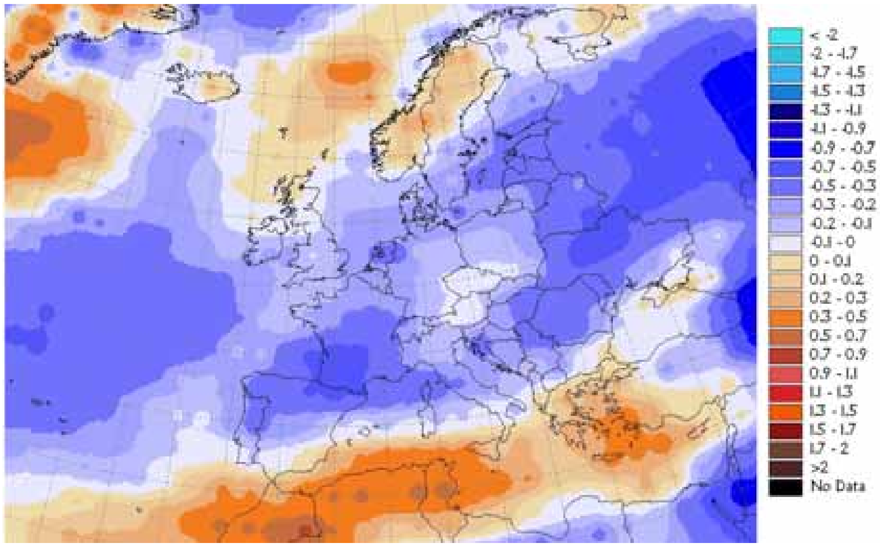

JJA

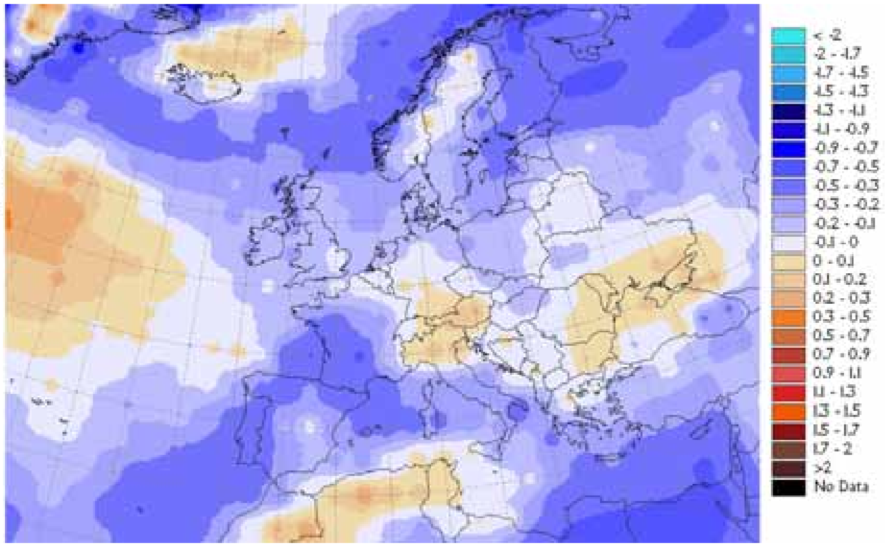

SON

Bias of the average of the yearly 10th percentile seasonal vorticity at 500hPa level (10^{-5}/s)

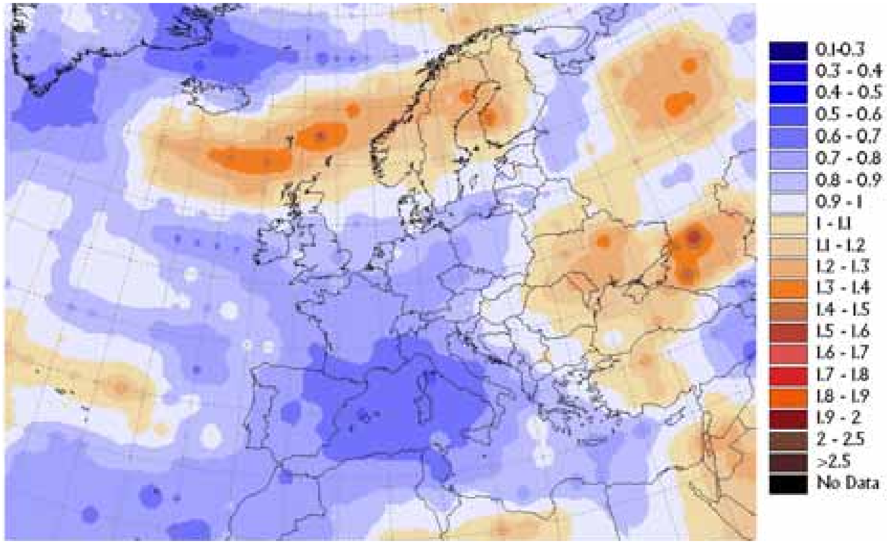

DJF

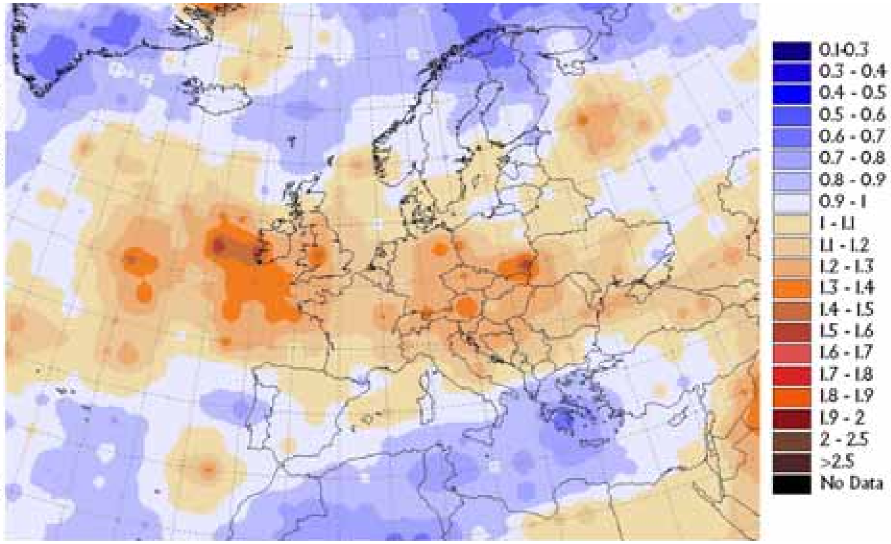

MAM

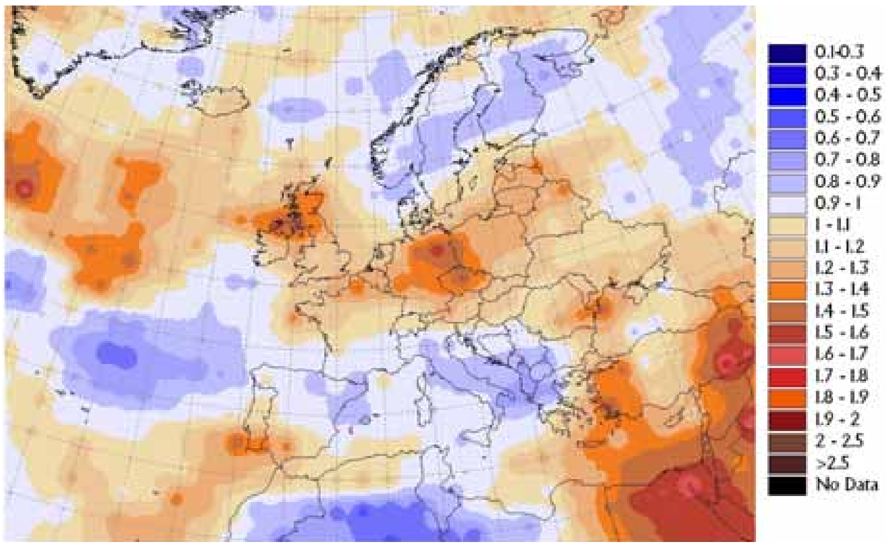

JJA

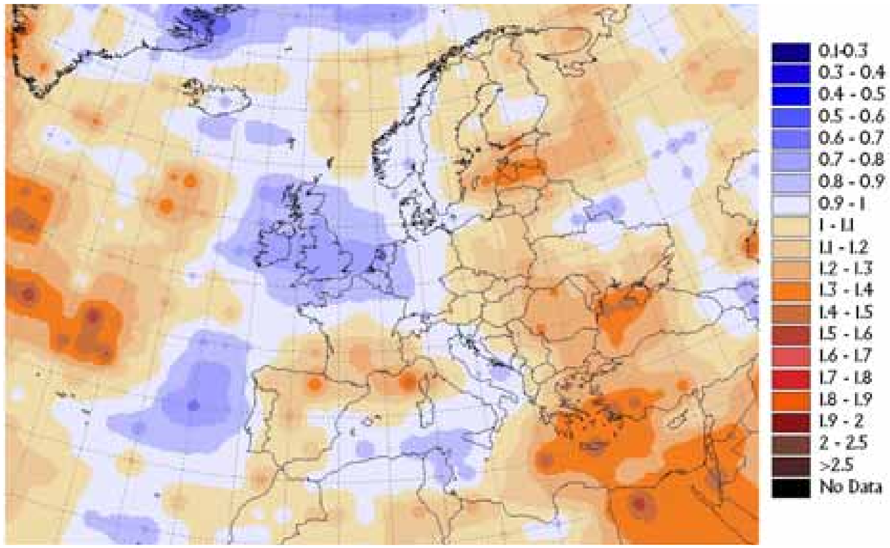

SON

Ratio of standard deviations of the yearly seasonal 10th percentile vorticity at 500hPa level

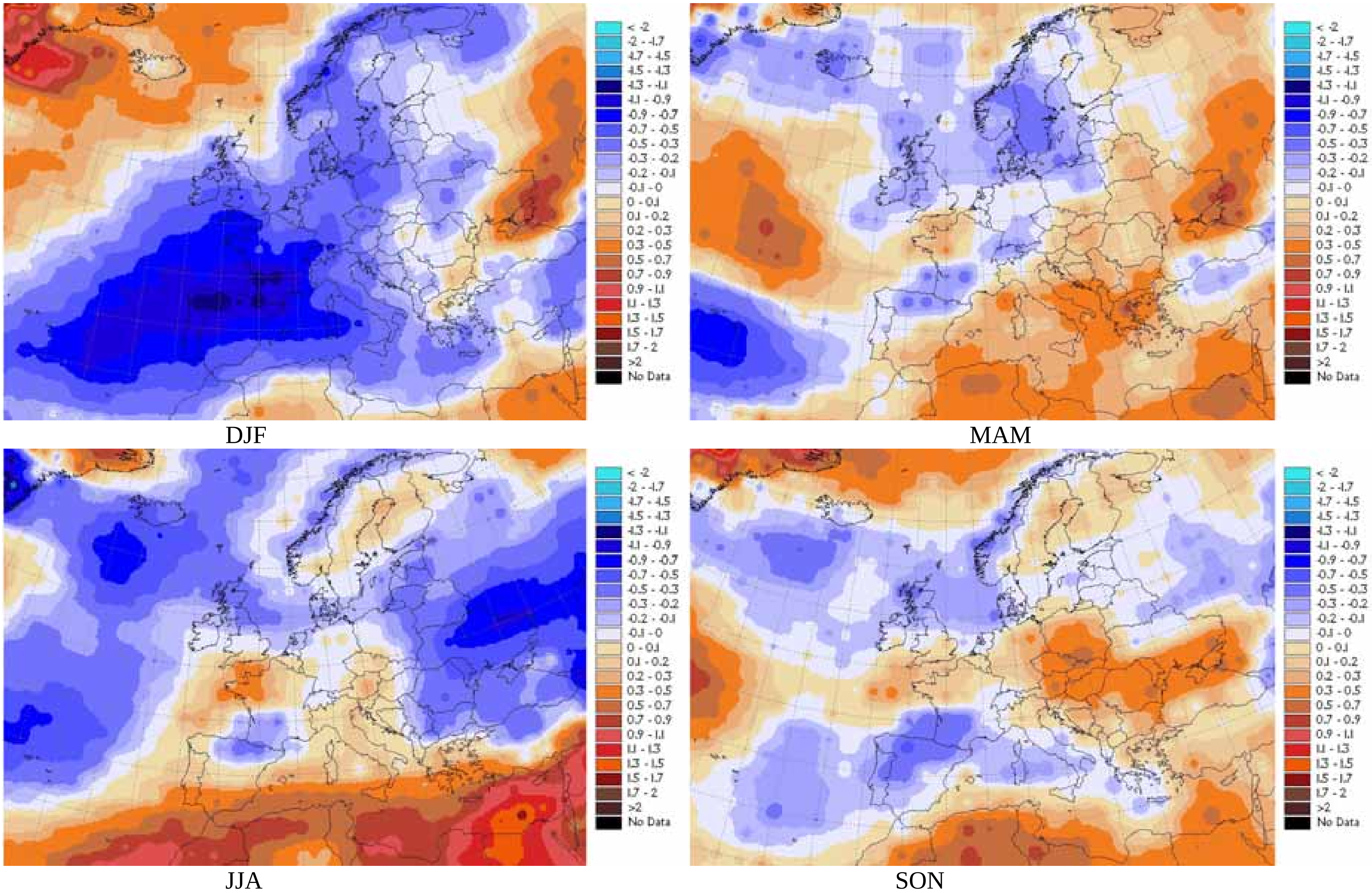

Bias of the average of the yearly 90th percentile seasonal vorticity at 500hPa level (10^{-5}/s)

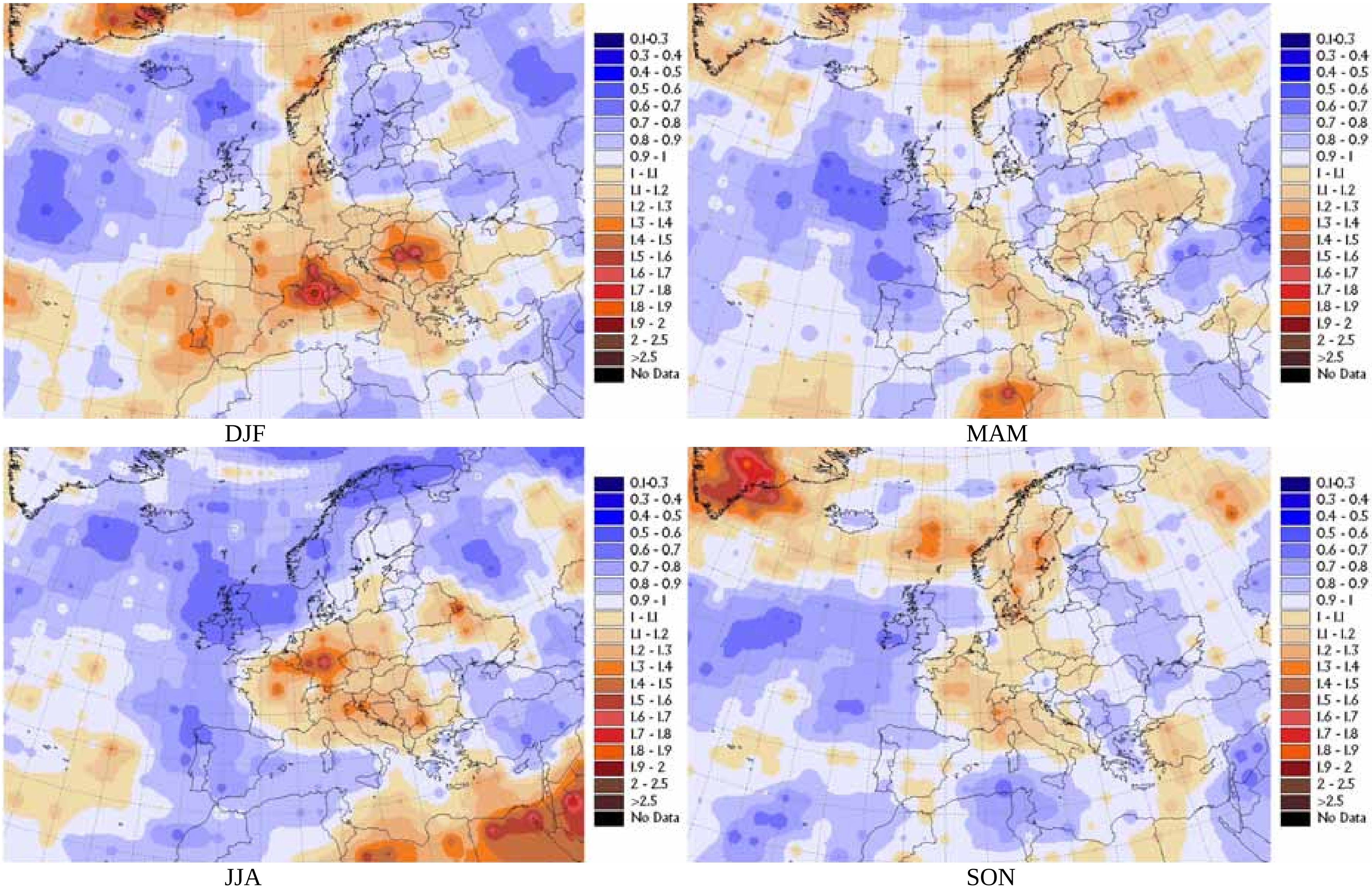

Ratio of standard deviations of the yearly seasonal 90th percentile vorticity at 500hPa level

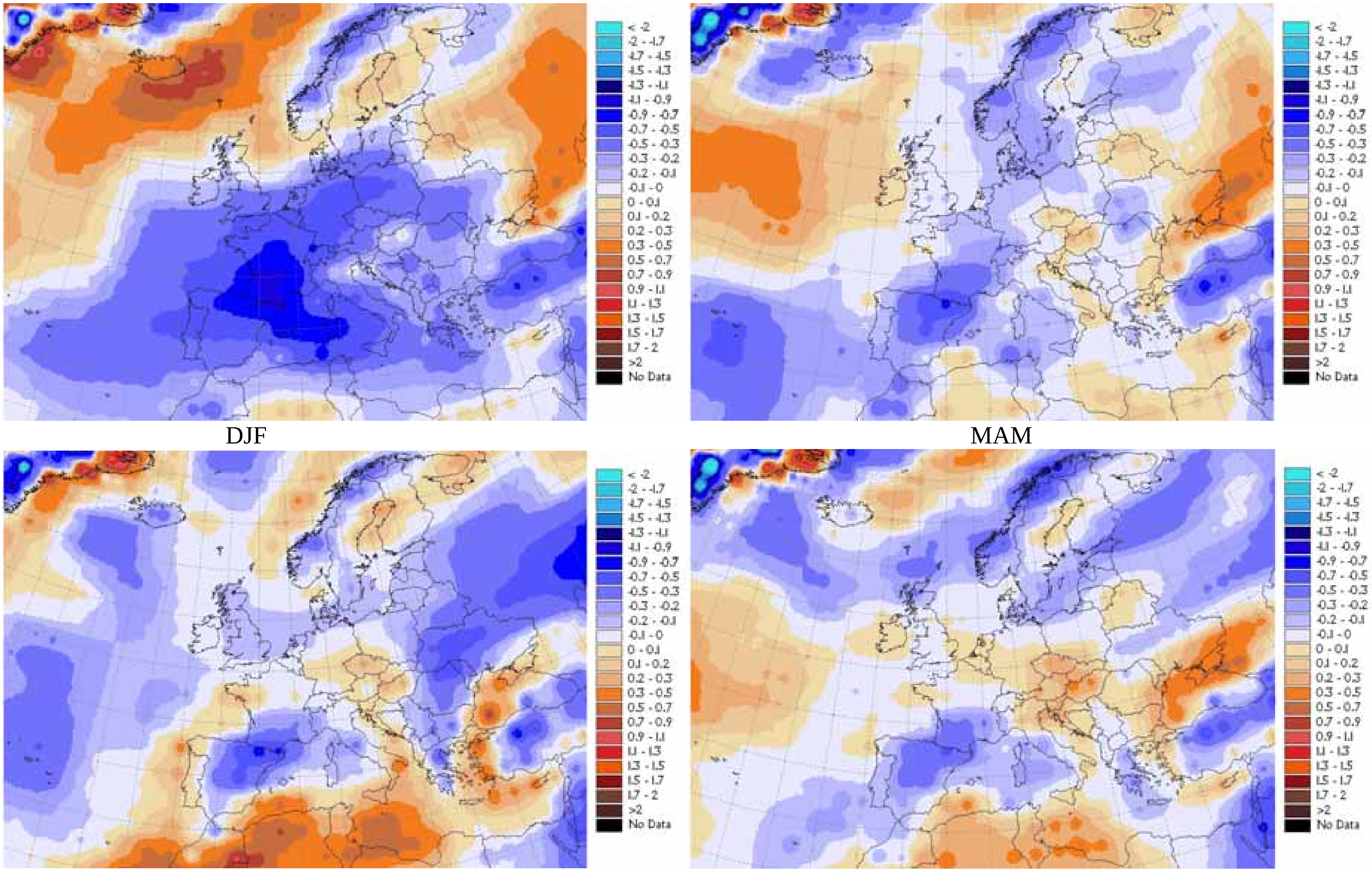

Bias of mean seasonal vorticity at 700hPa level (10^{-5}/s)

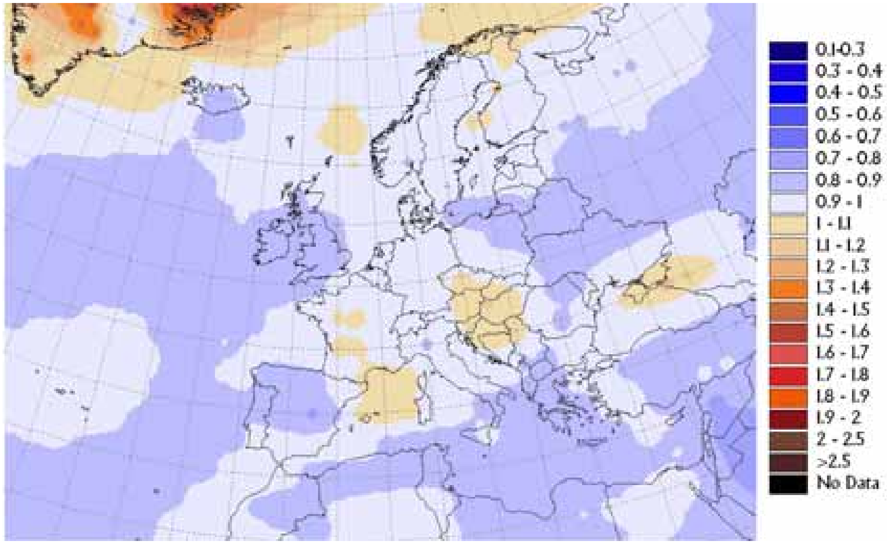

DJF

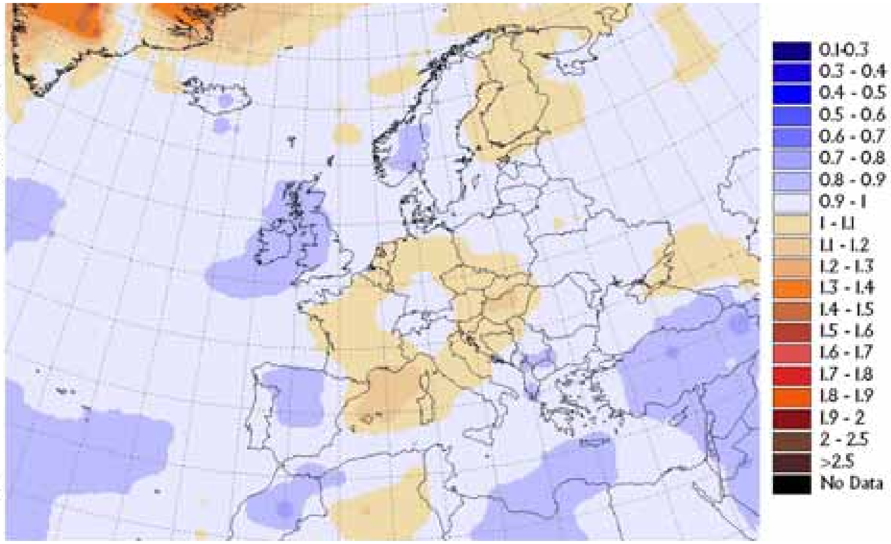

MAM

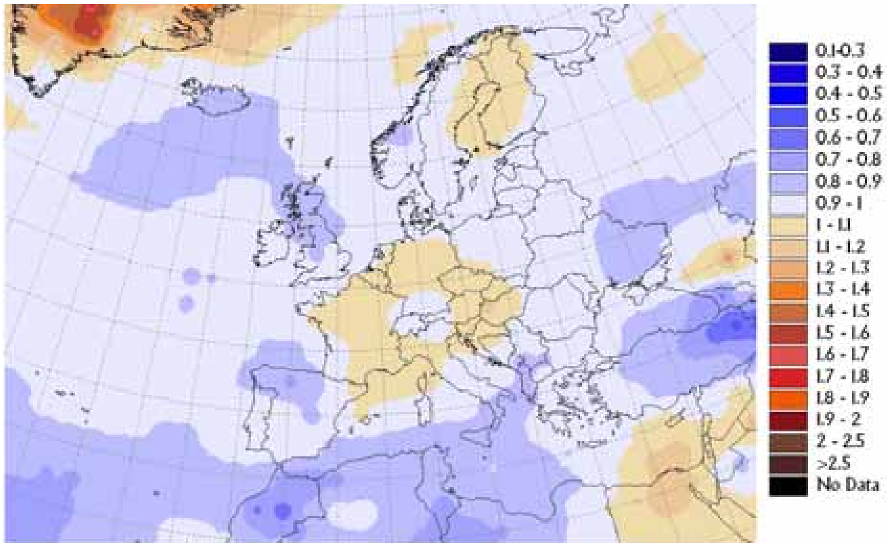

JJA

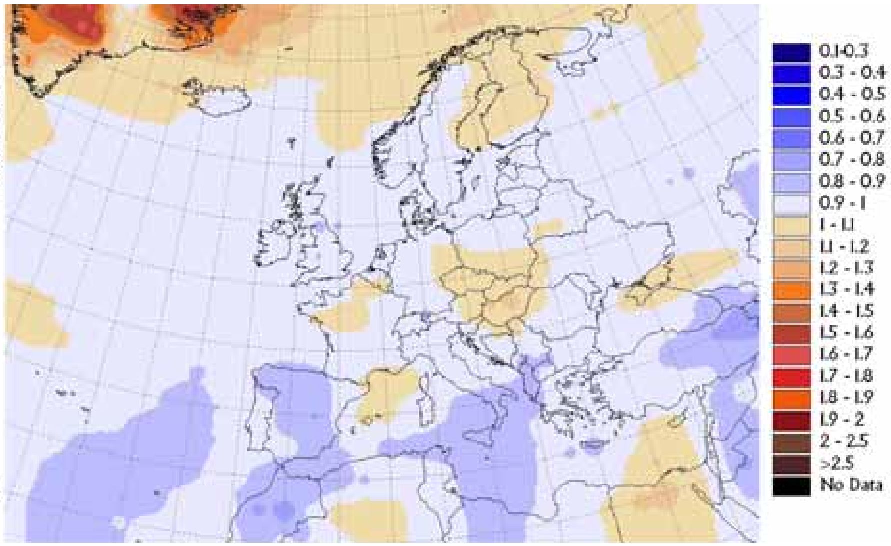

SON

Ratio of standard deviations of daily values of vorticity at 700hPa level

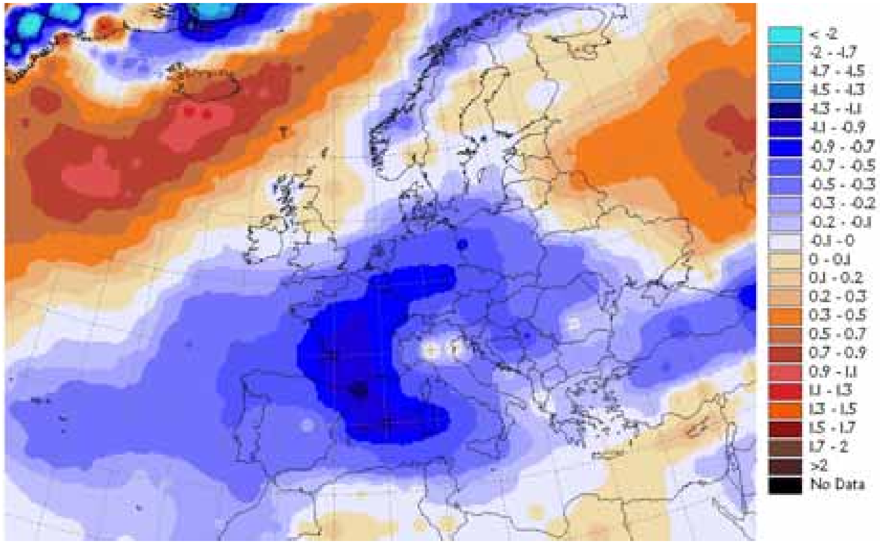

DJF

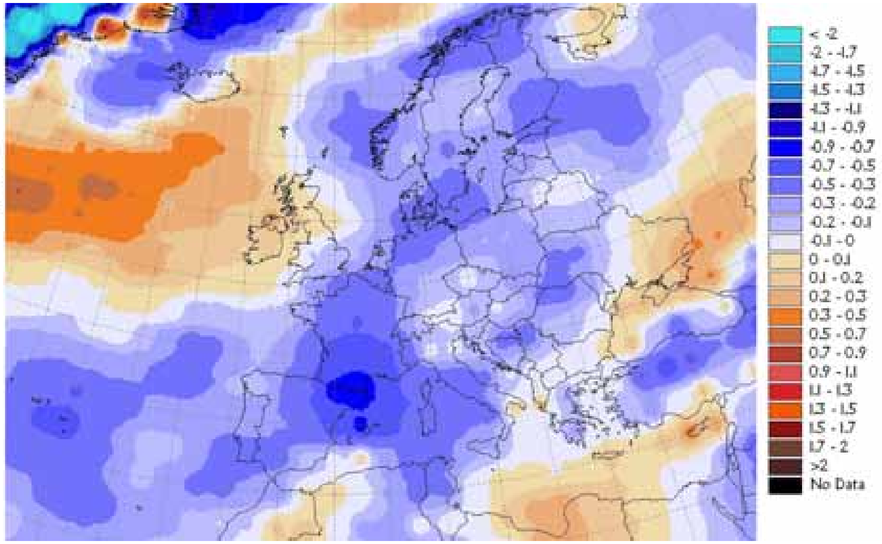

MAM

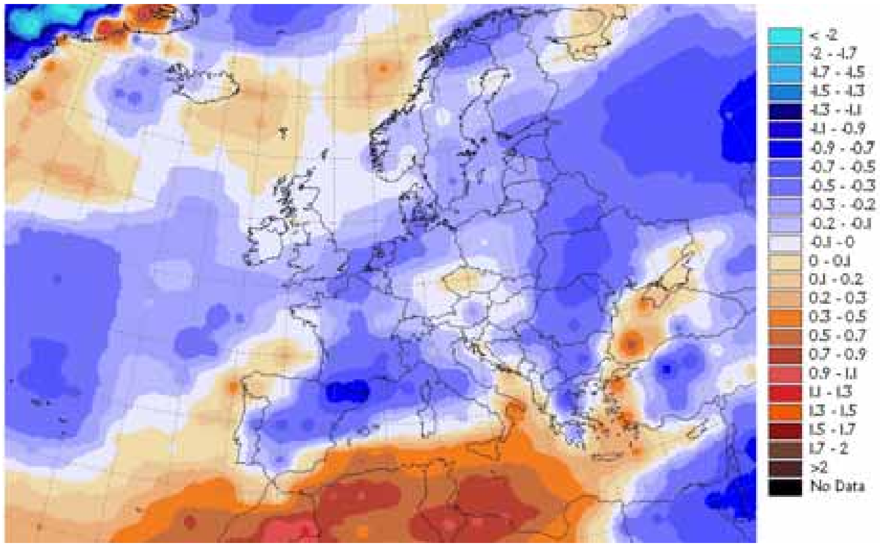

JJA

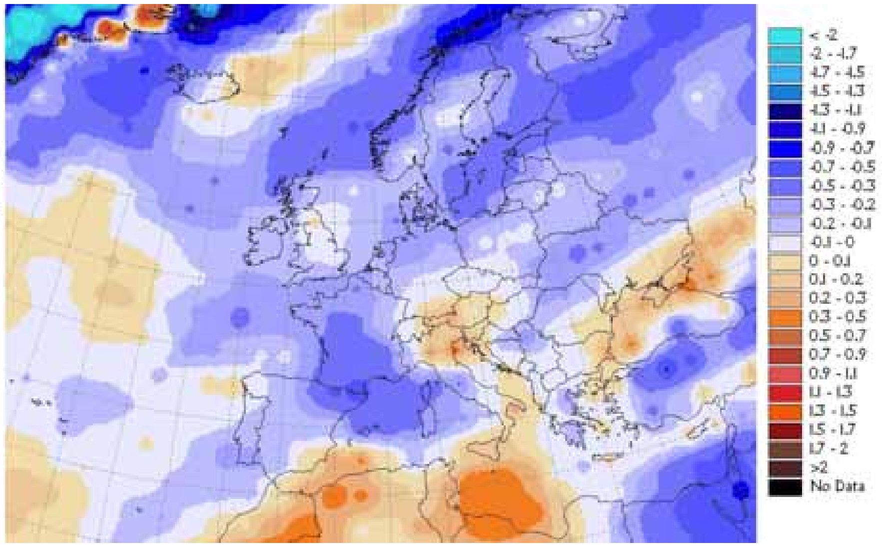

SON

Bias of the average of the yearly 10th percentile seasonal vorticity at 700hPa level (10^{-5}/s)

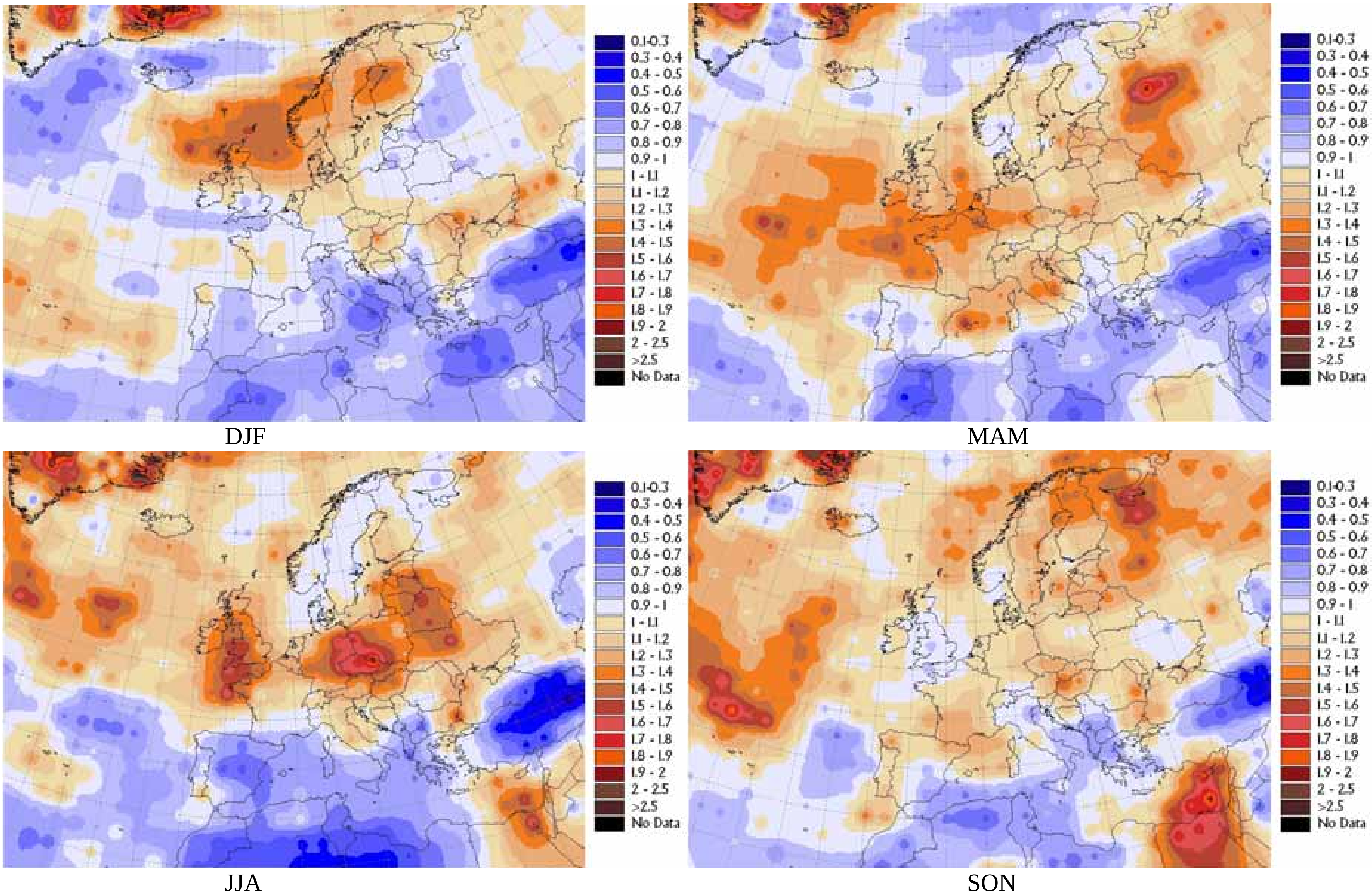

Ratio of standard deviations of the yearly seasonal 10th percentile vorticity at 700hPa level

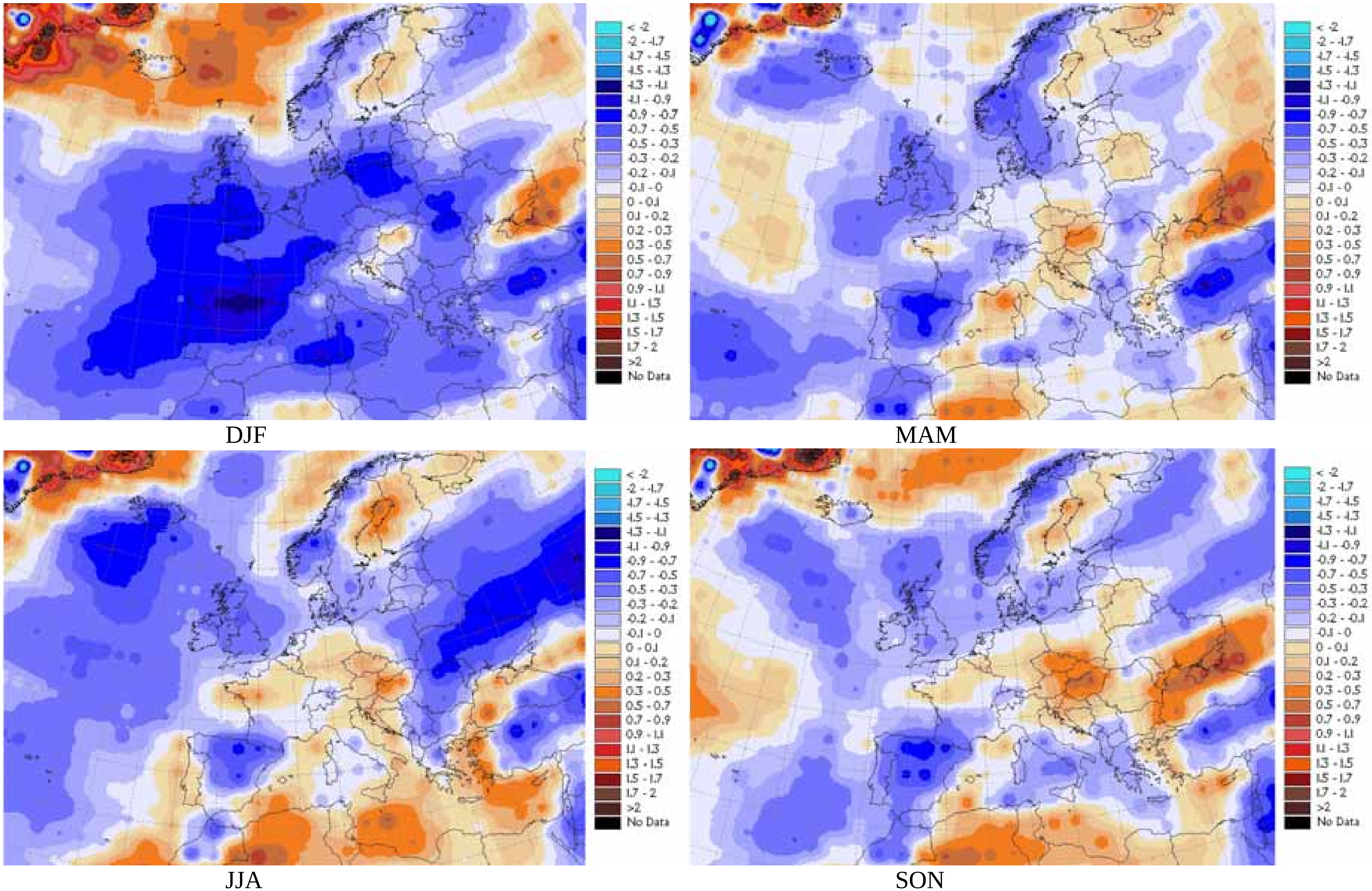

Bias of the average of the yearly 90th percentile seasonal vorticity at 700hPa level (10^{-5}/s)

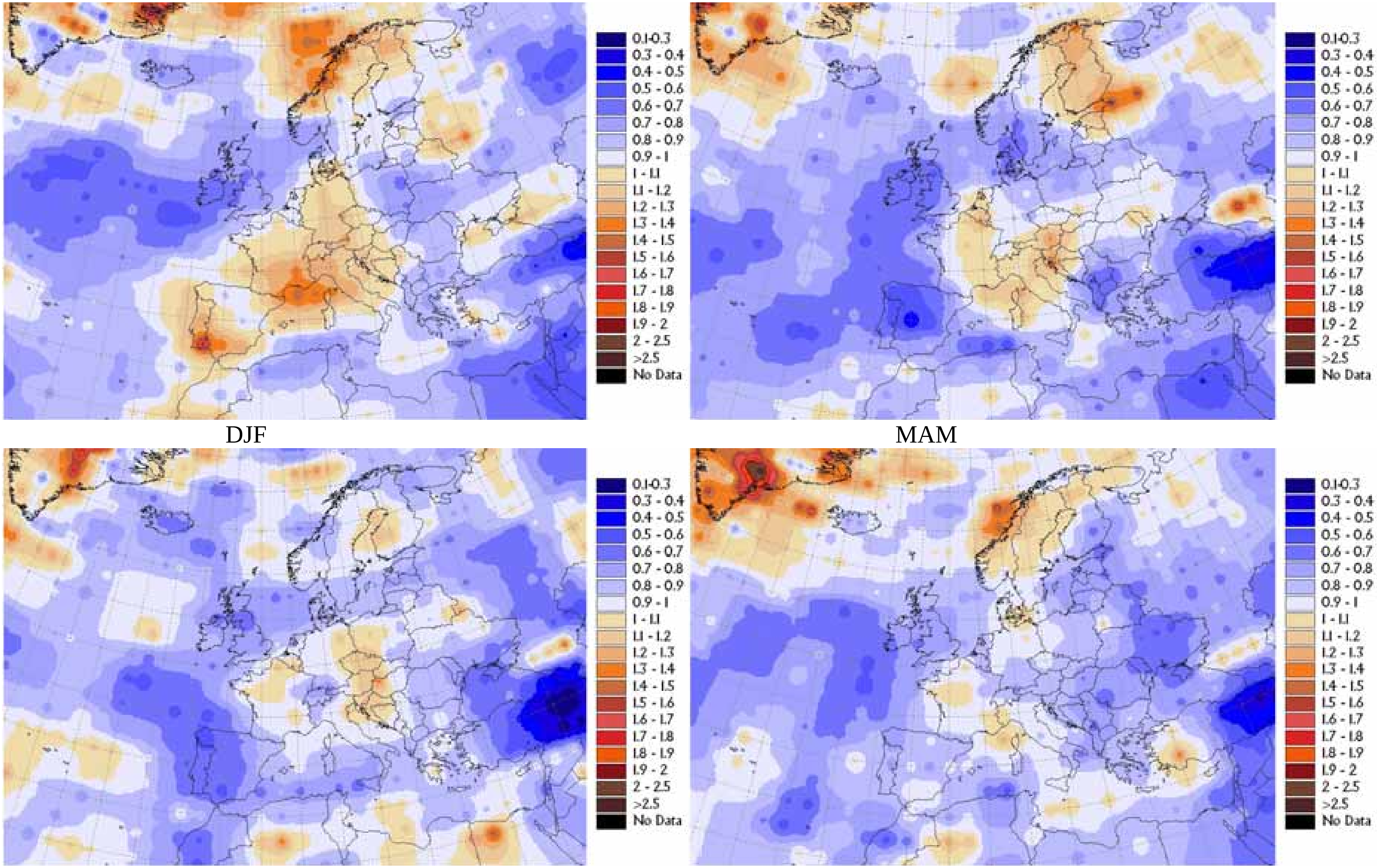

DJF MAM

JJA SON

Ratio of standard deviations of the yearly seasonal 90th percentile vorticity at 700hPa level

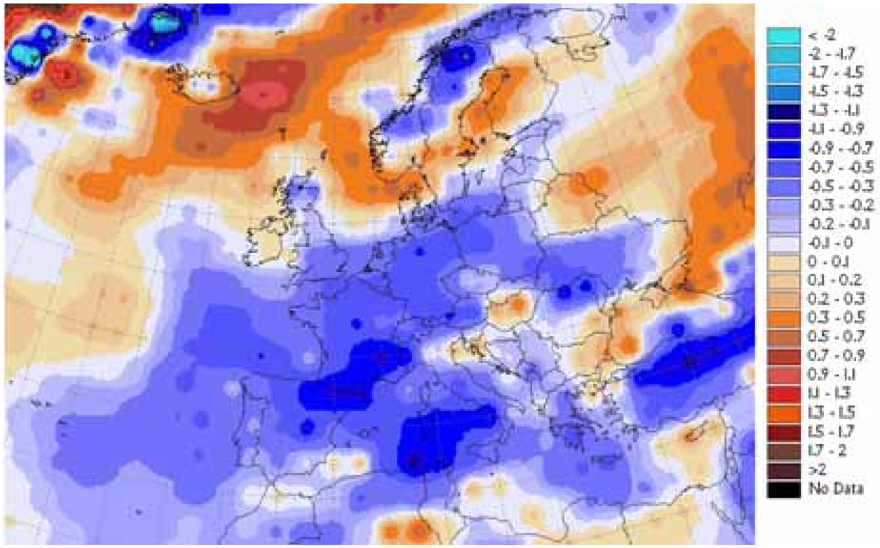

DJF

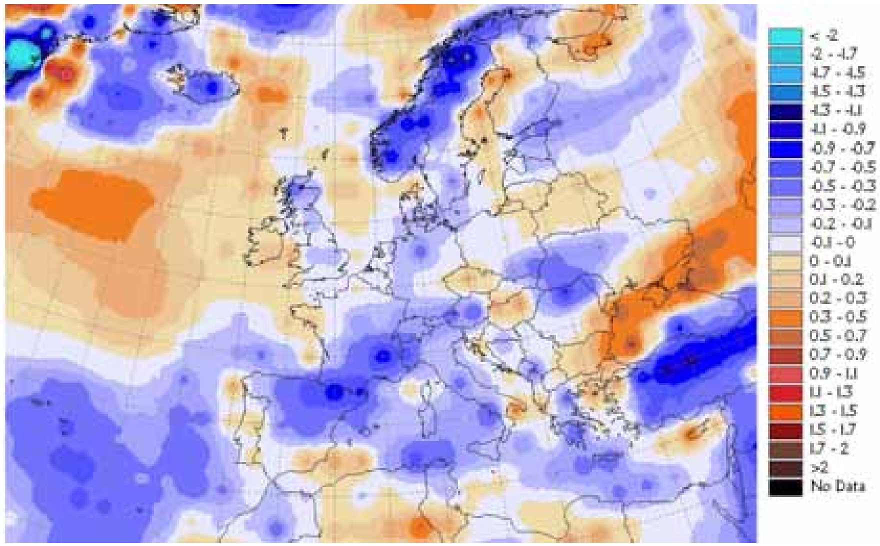

MAM

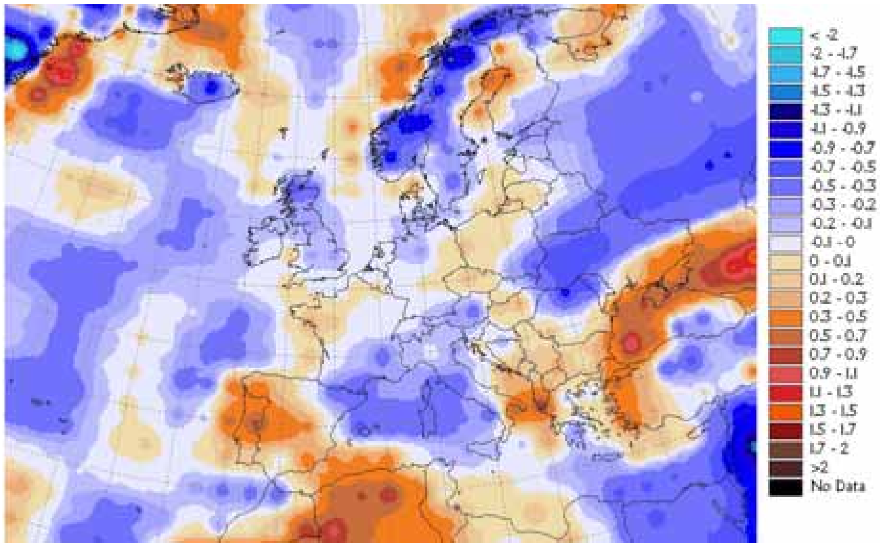

JJA

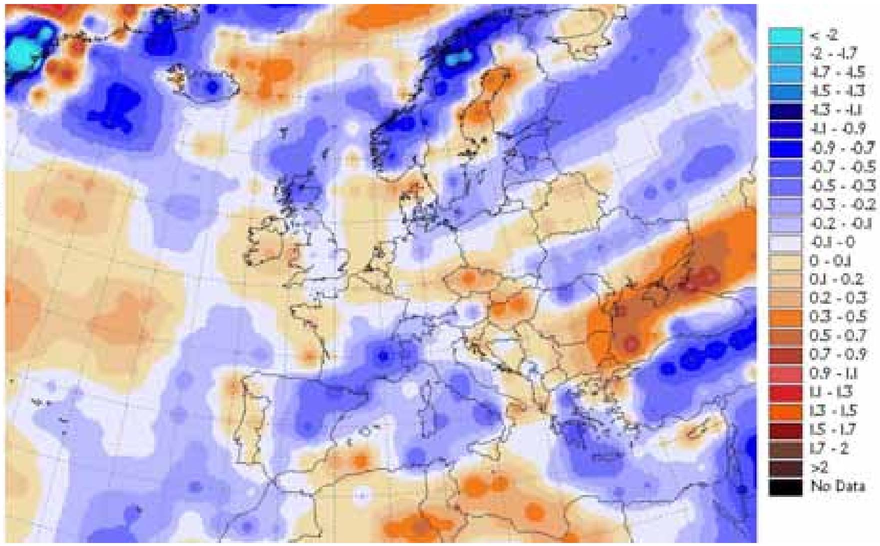

SON

Bias of mean seasonal vorticity at 850hPa level (10^{-5}/s)

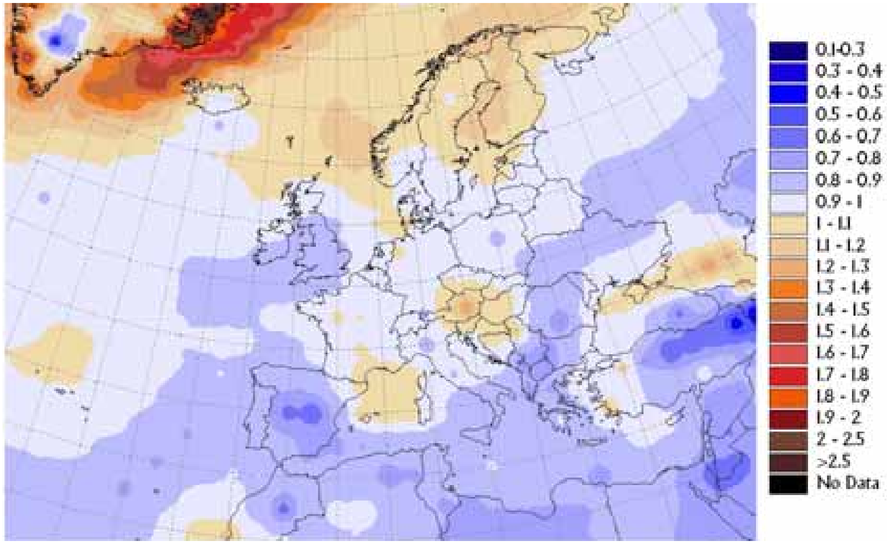

DJF

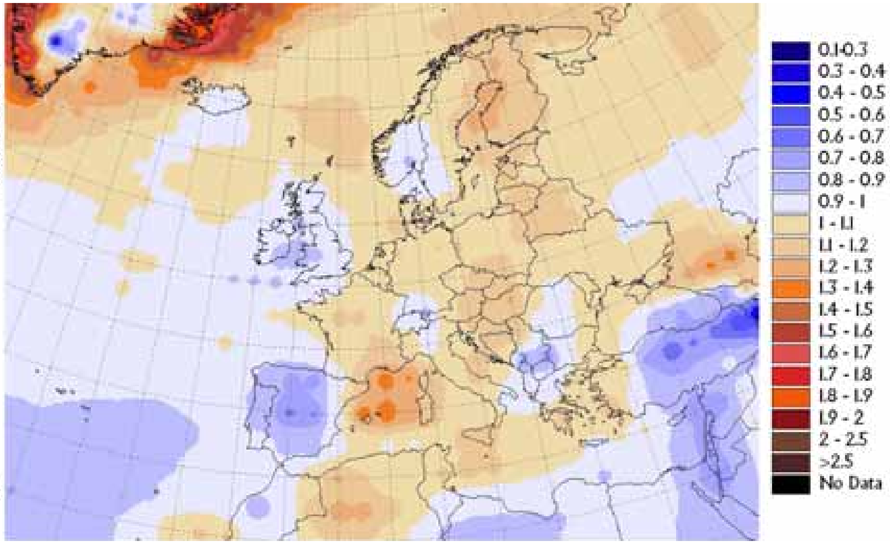

MAM

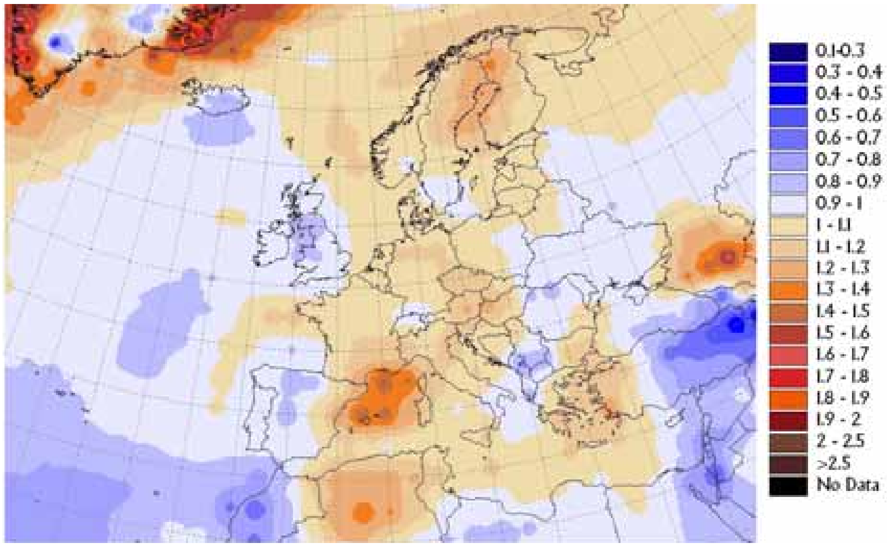

JJA

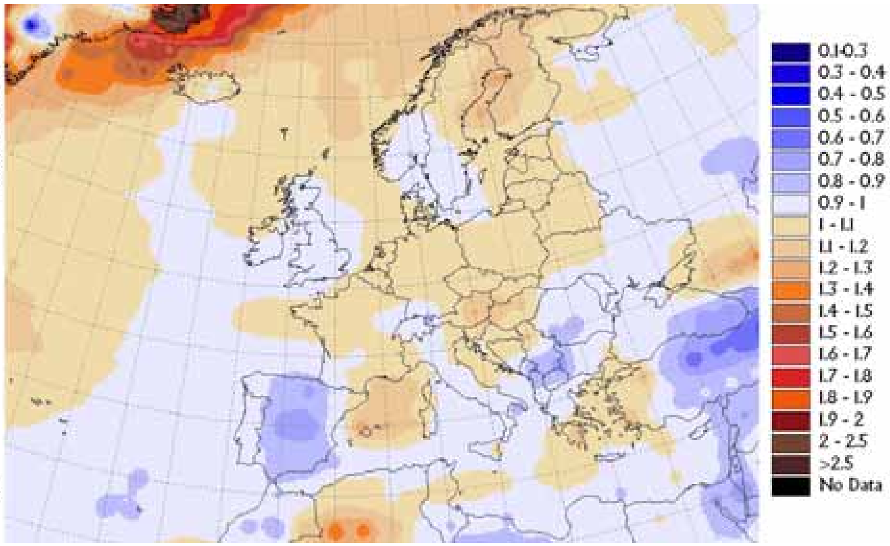

SON

Ratio of standard deviations of daily values of vorticity at 850hPa level

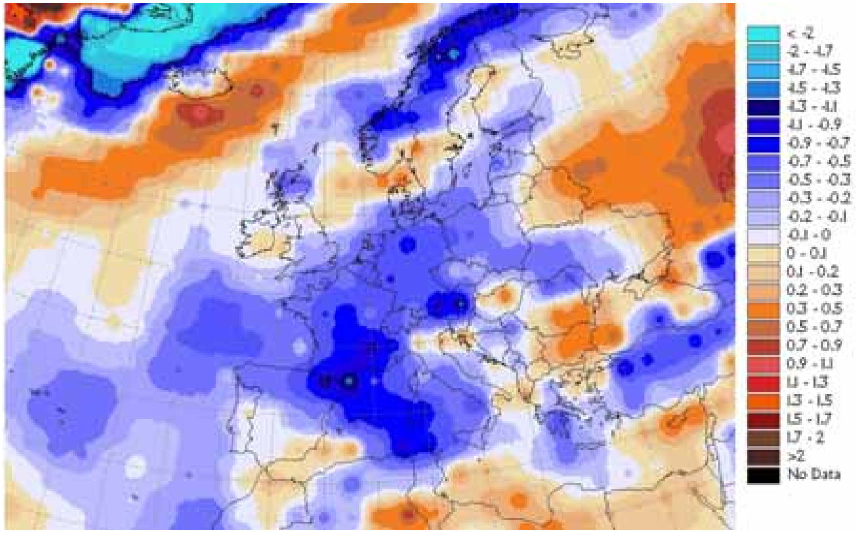

DJF

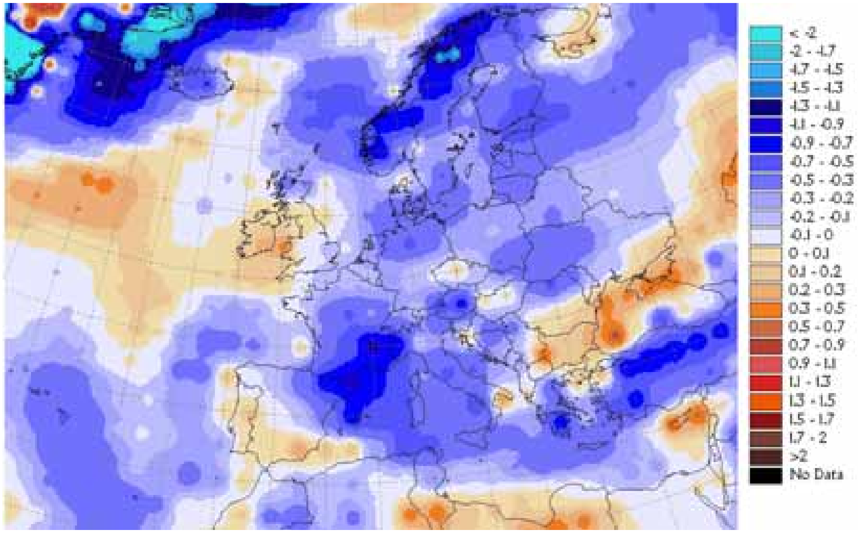

MAM

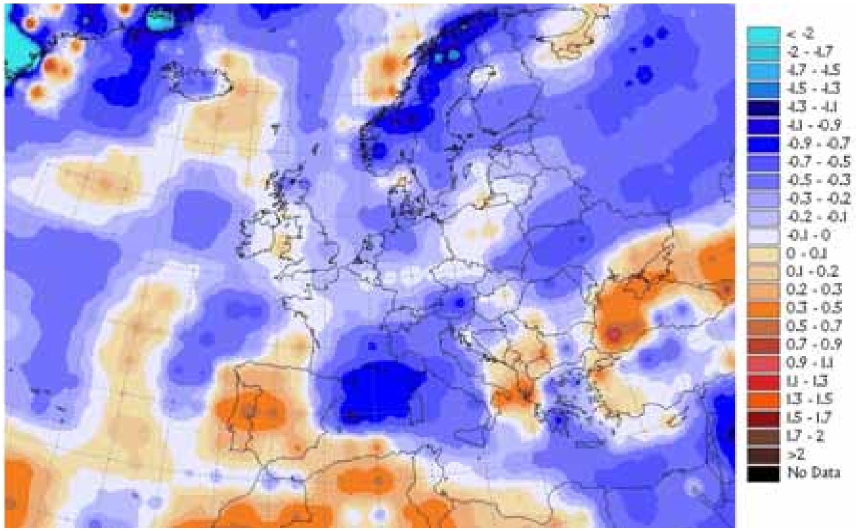

JJA

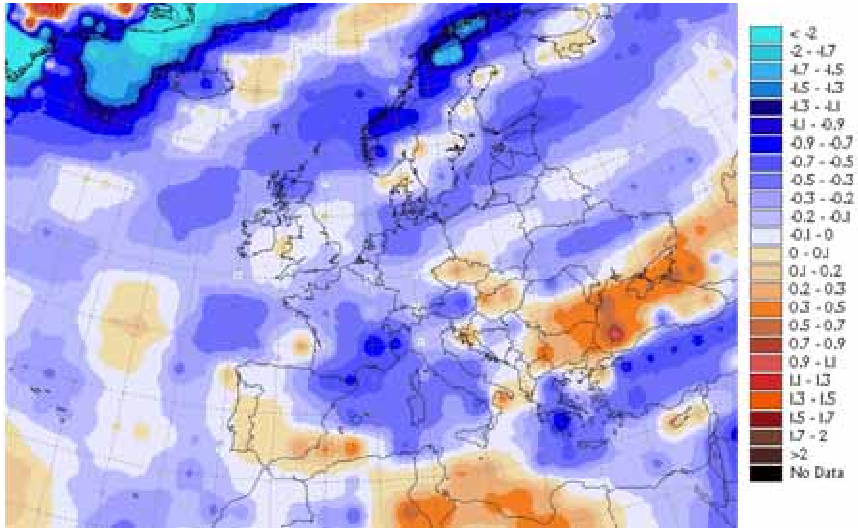

SON

Bias of the average of the yearly 10th percentile seasonal vorticity at 850hPa level (10^{-5}/s)

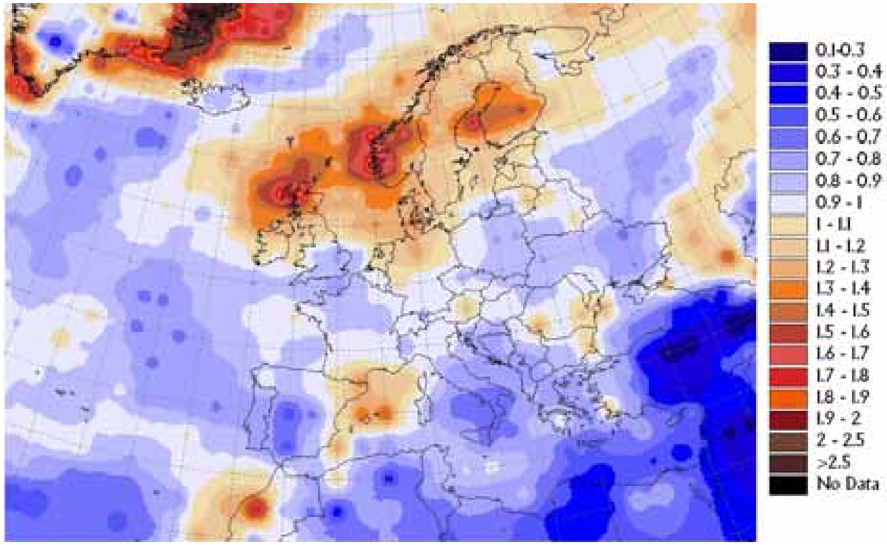

DJF

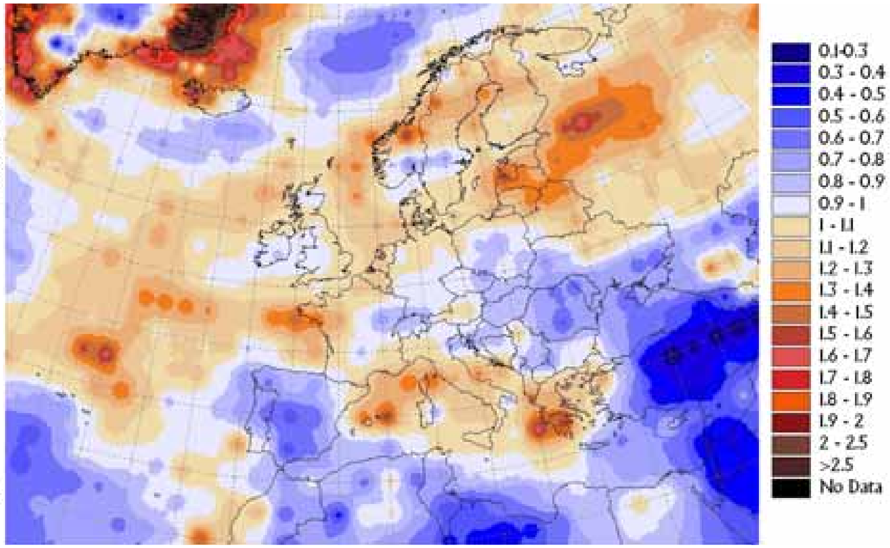

MAM

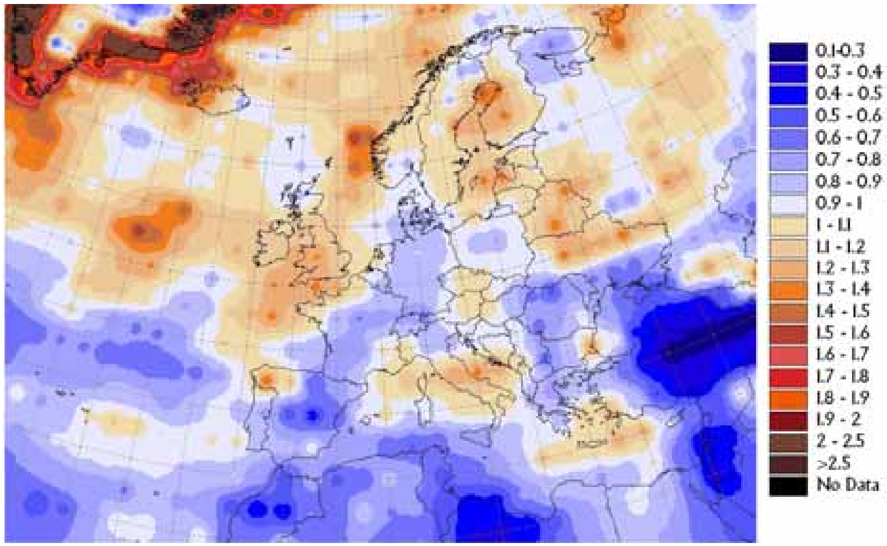

JJA

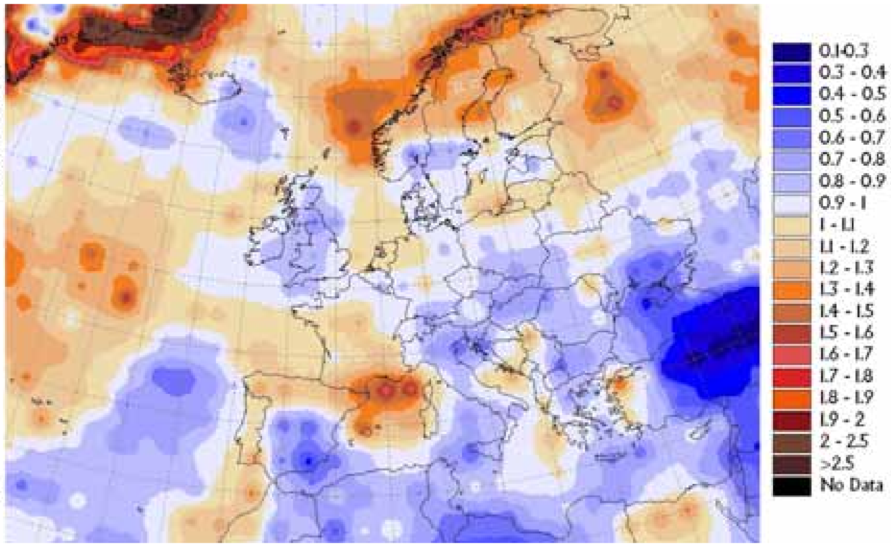

SON

Ratio of standard deviations of the yearly seasonal 10th percentile vorticity at 850hPa level

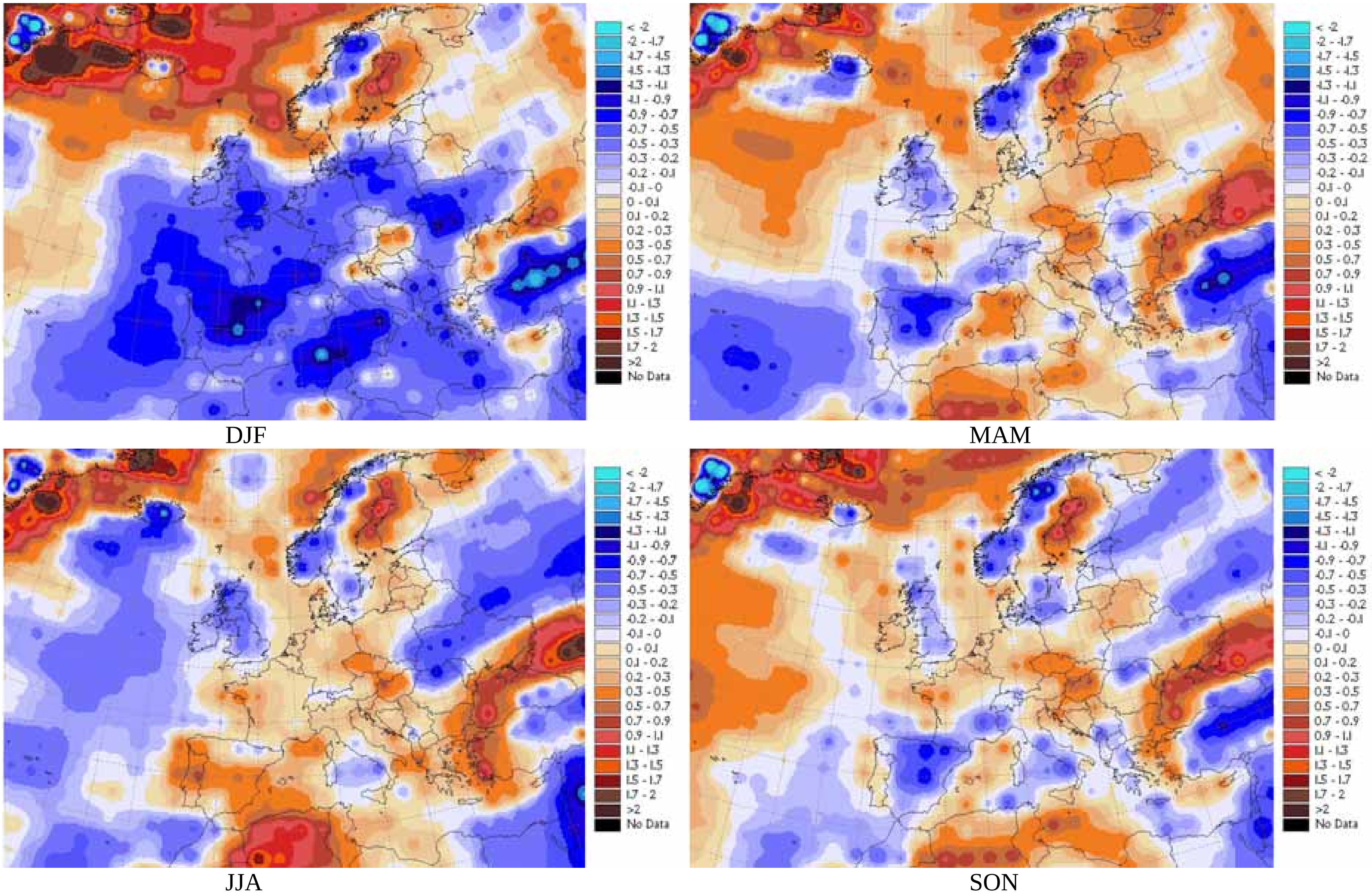

Bias of the average of the yearly 90th percentile seasonal vorticity at 850hPa level (10^{-5}/s)

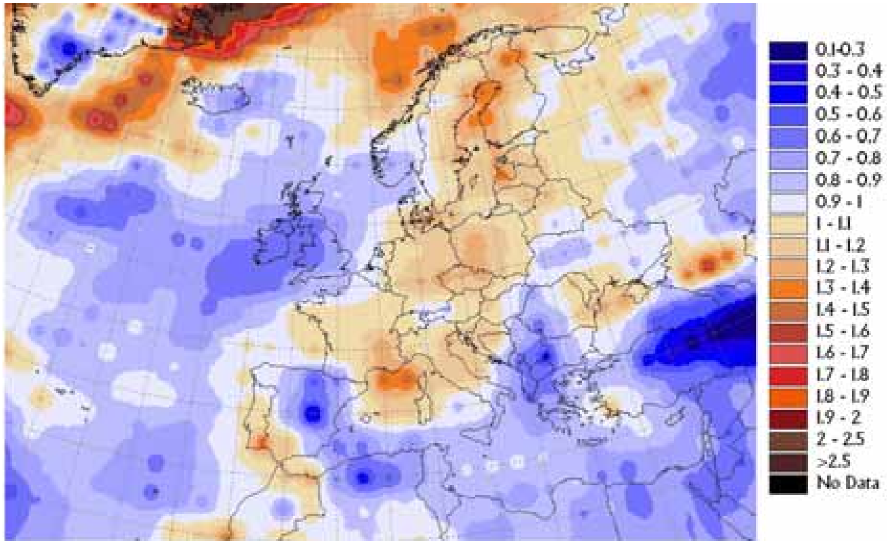

DJF

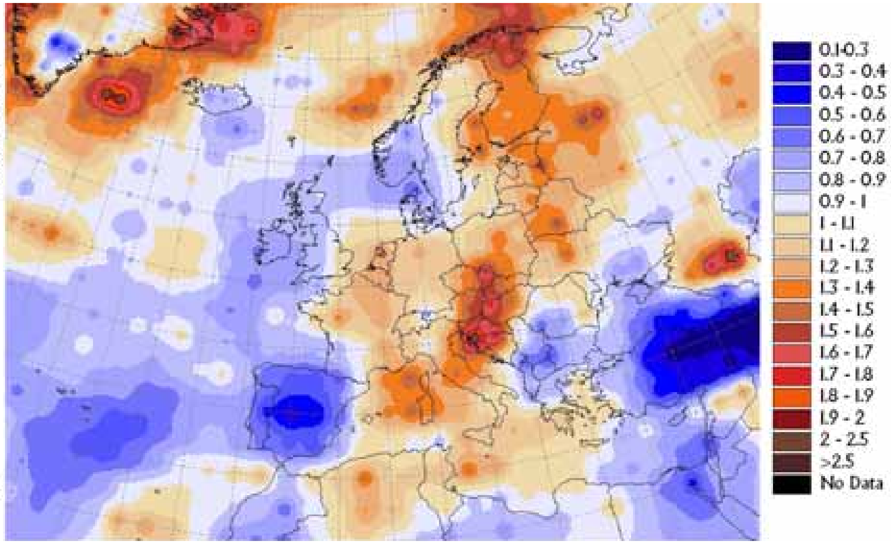

MAM

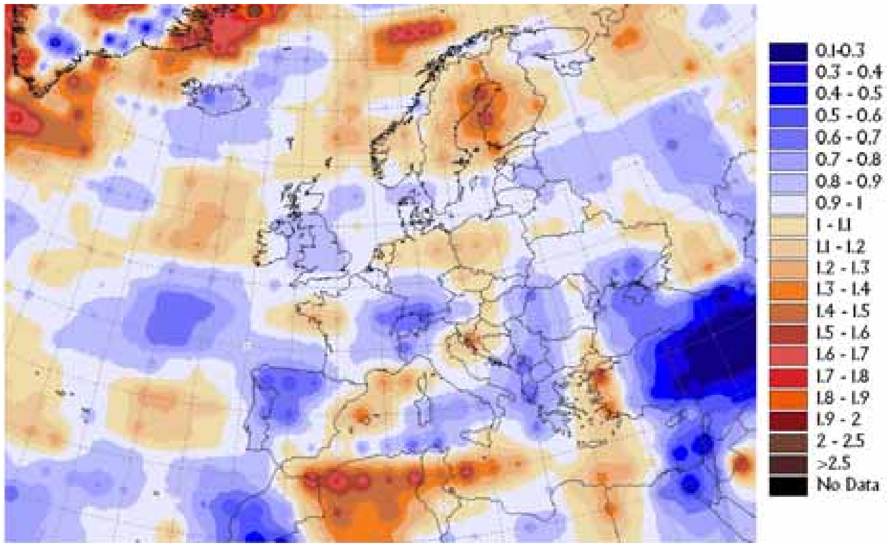

JJA

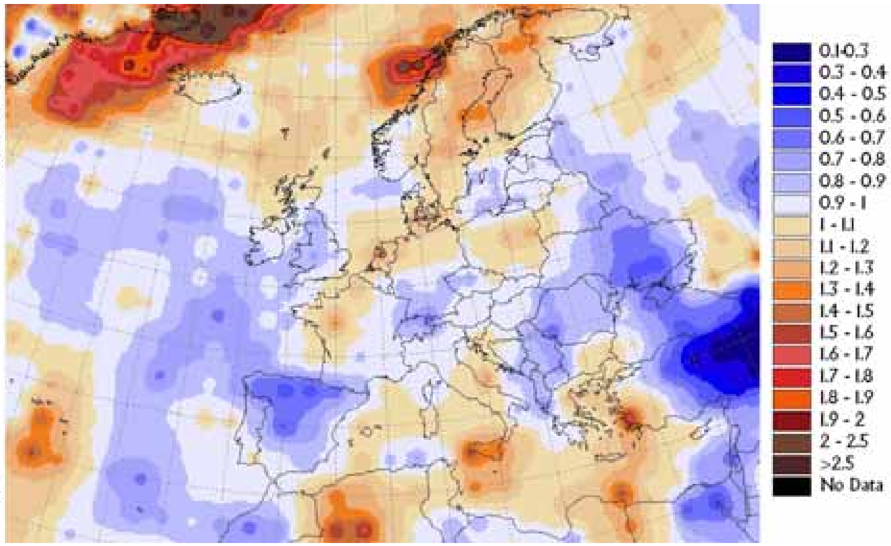

SON

Ratio of standard deviations of the yearly seasonal 90th percentile vorticity at 850hPa level

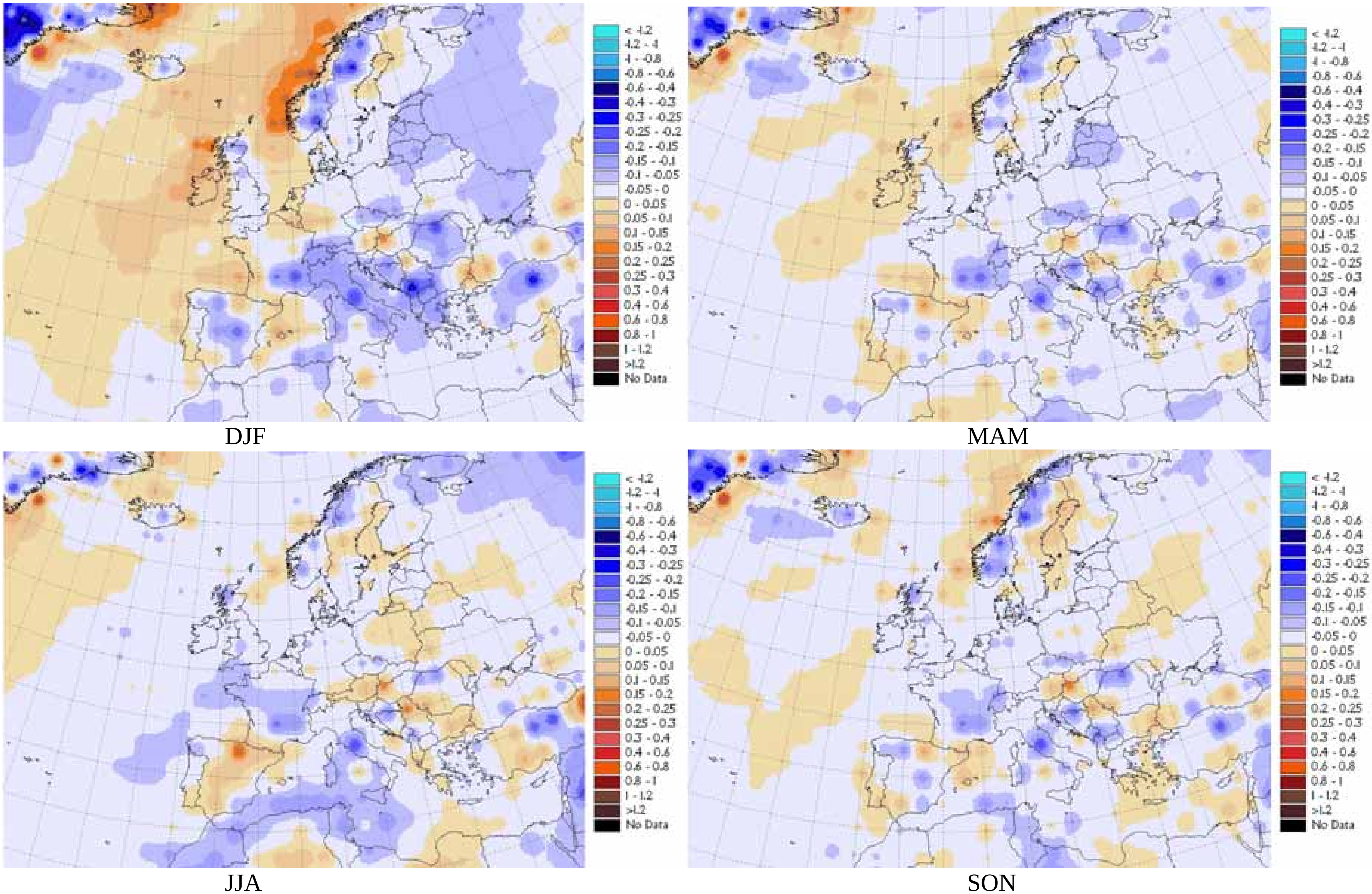

Bias of mean seasonal divergence at 500hPa level (10^{-5}/s)

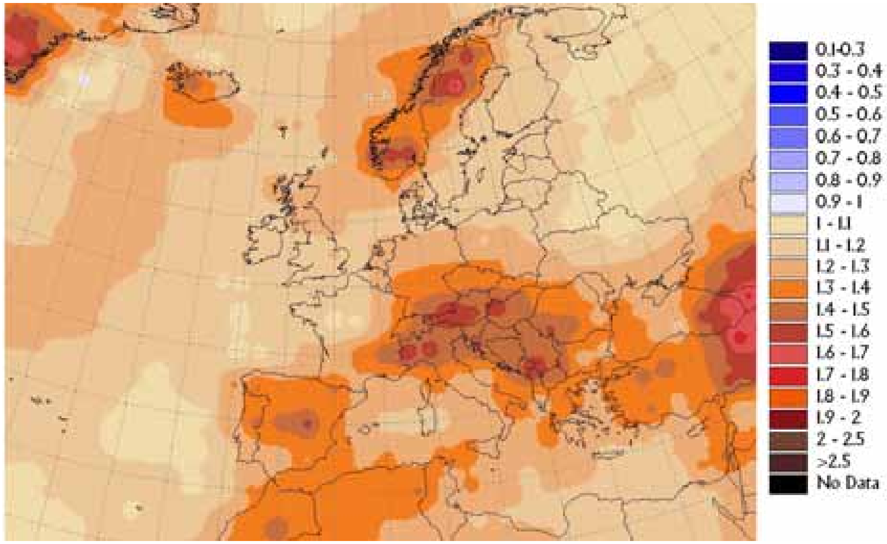

DJF

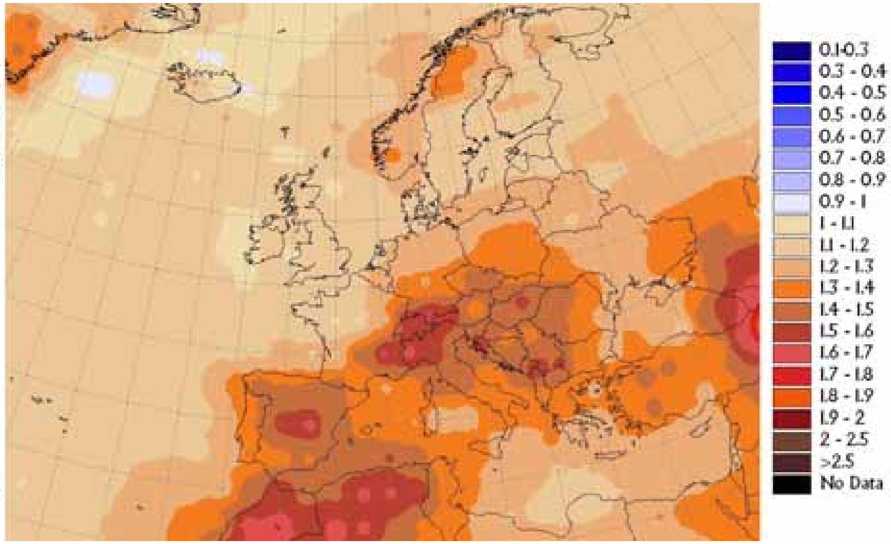

MAM

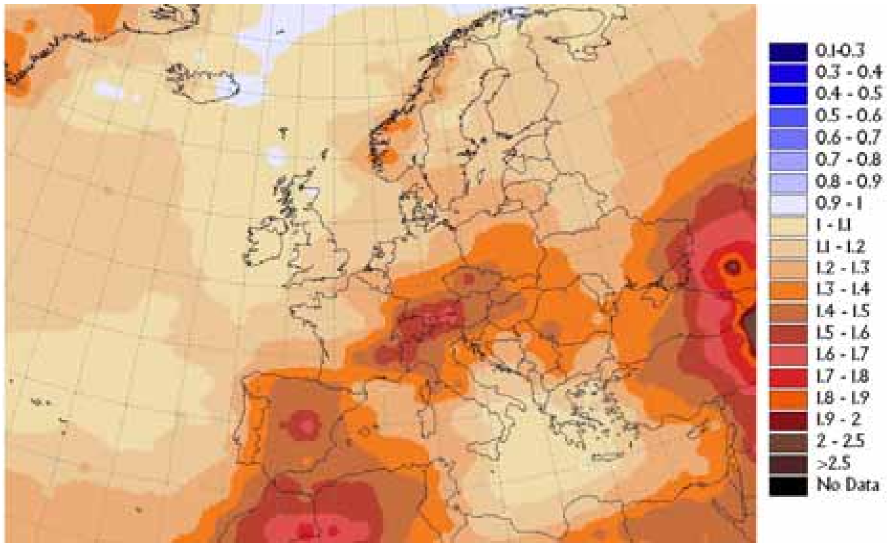

JJA

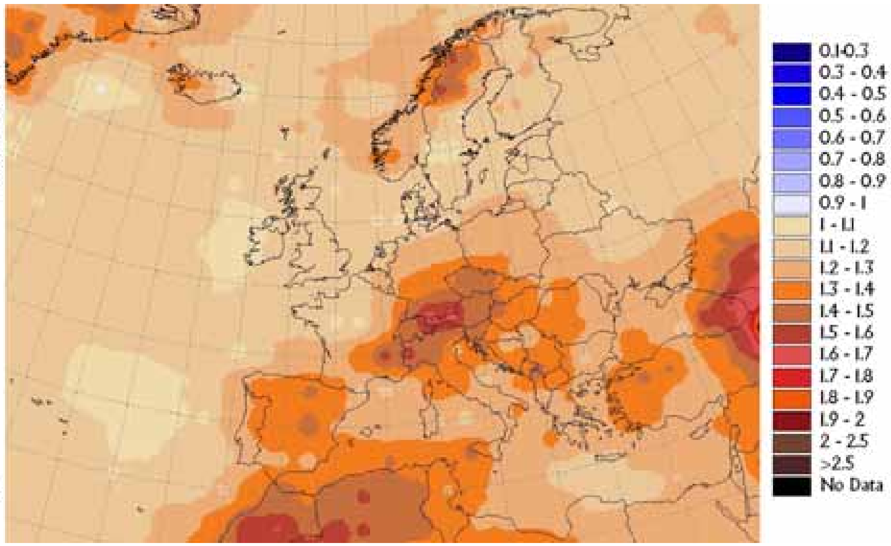

SON

Ratio of standard deviations of daily values of divergence at 500hPa level

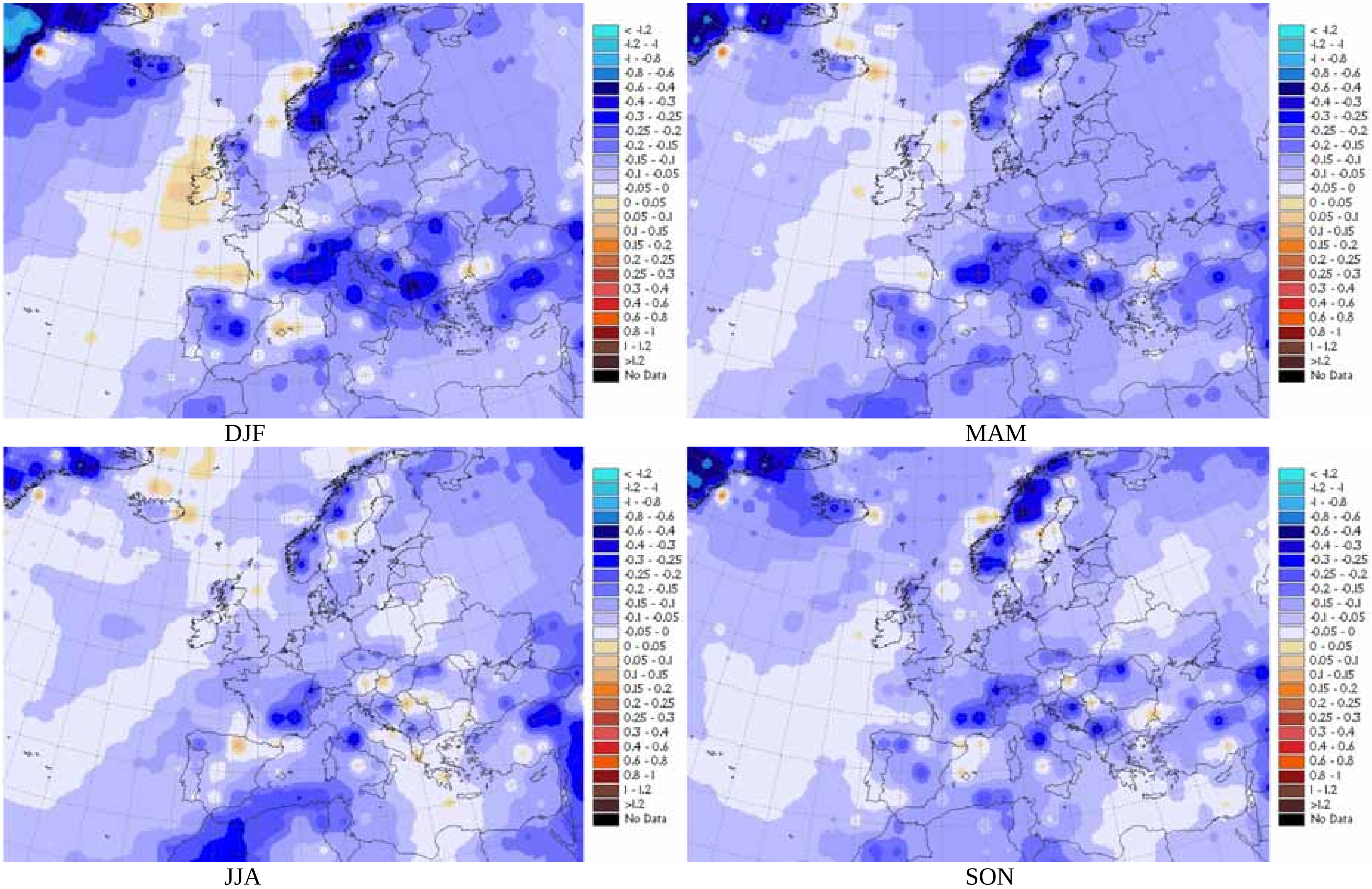

Bias of the average of the yearly 10th percentile seasonal divergence at 500hPa level (10^{-5}/s)

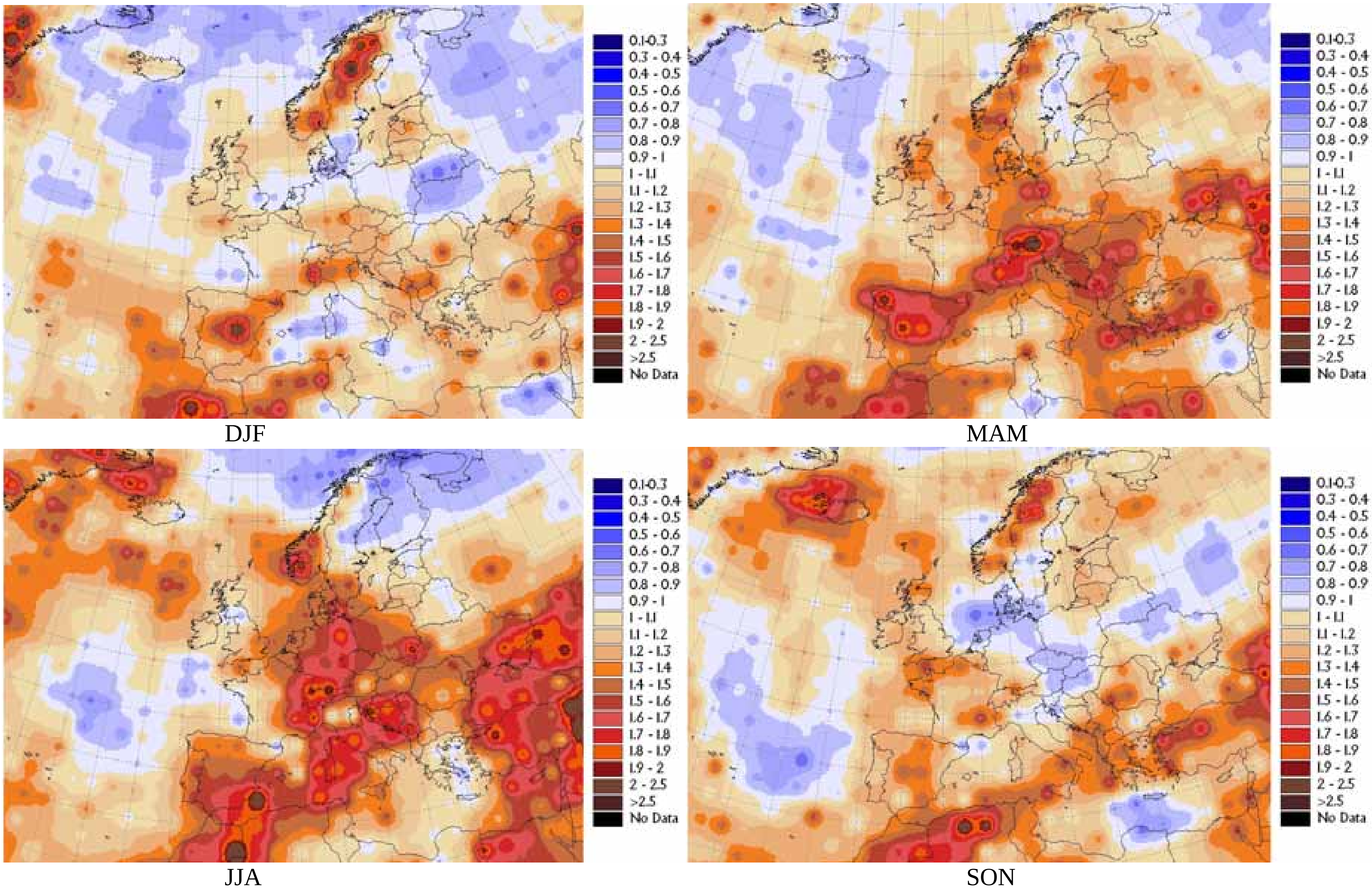

Ratio of standard deviations of the yearly seasonal 10th percentile divergence at 500hPa level

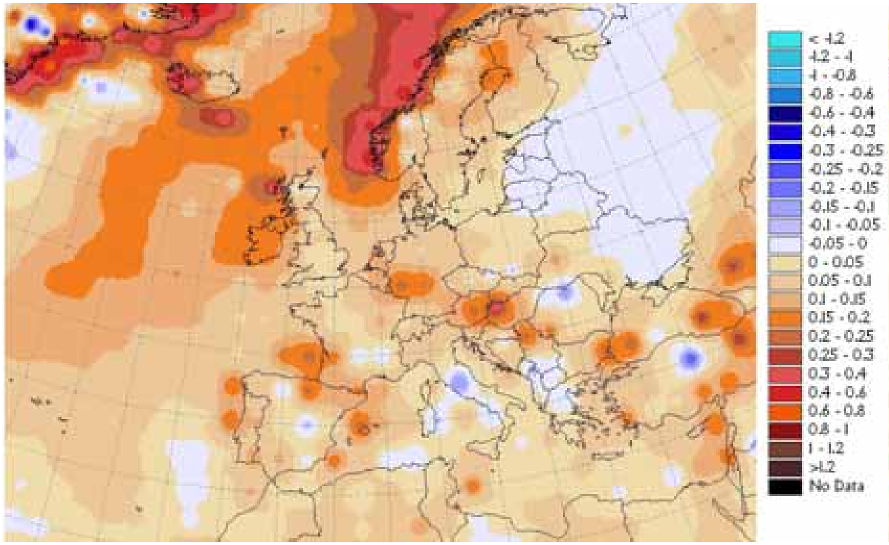

DJF

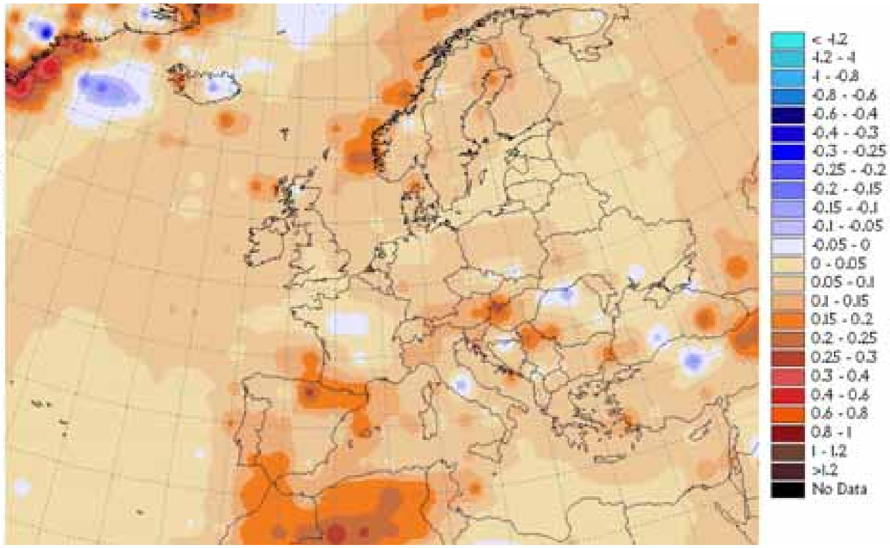

MAM

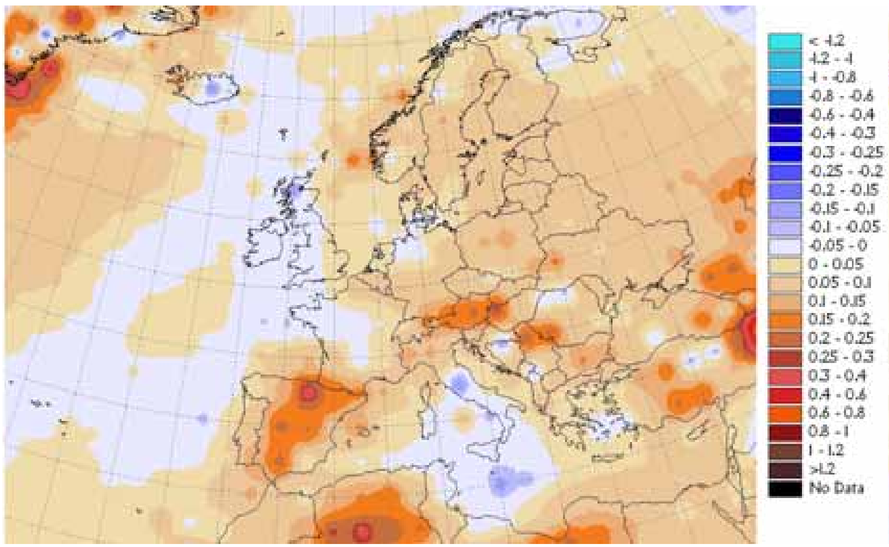

JJA

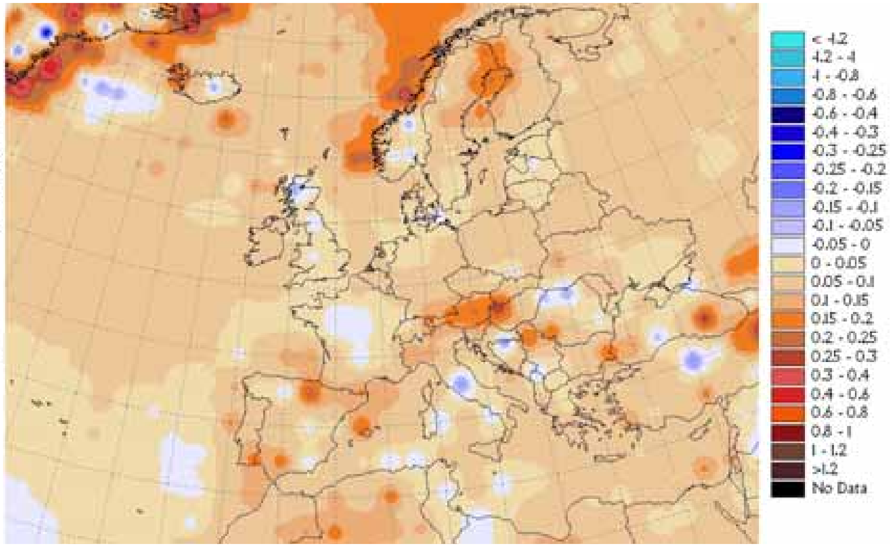

SON

Bias of the average of the yearly 90th percentile seasonal divergence at 500hPa level (10^{-5}/s)

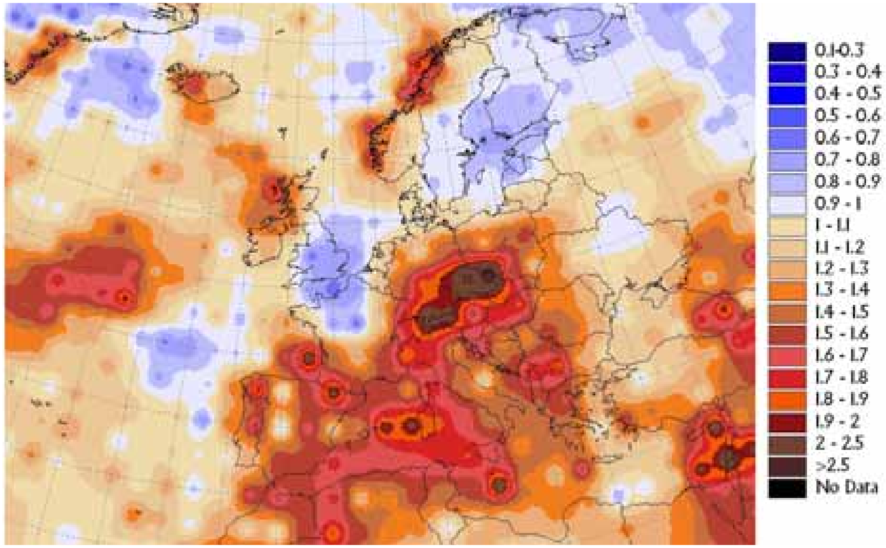

DJF

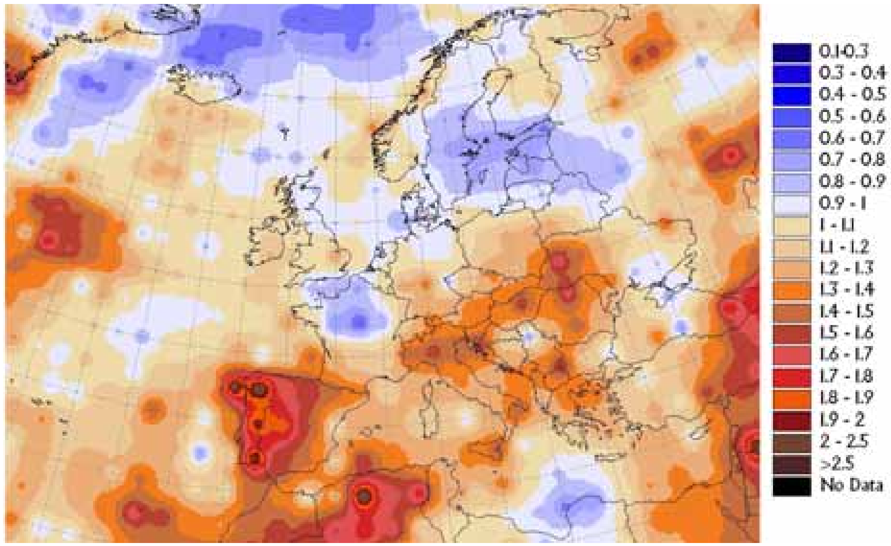

MAM

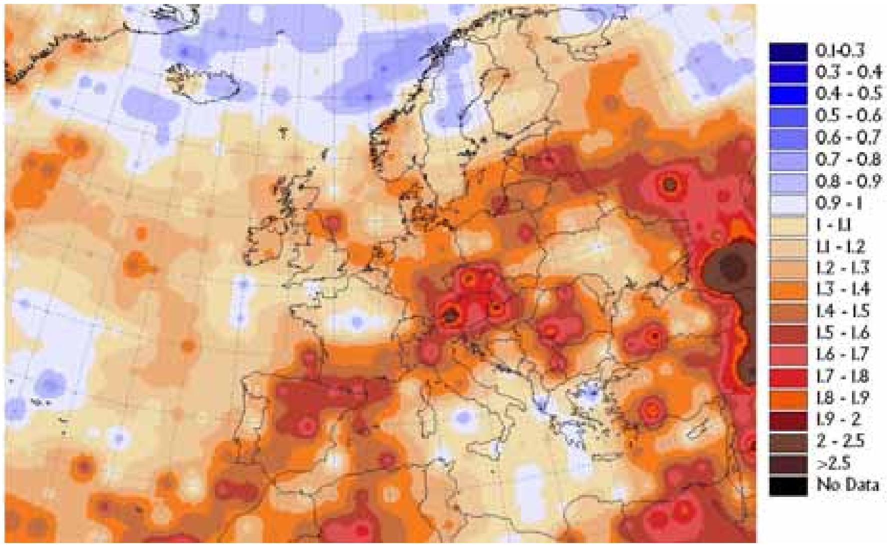

JJA

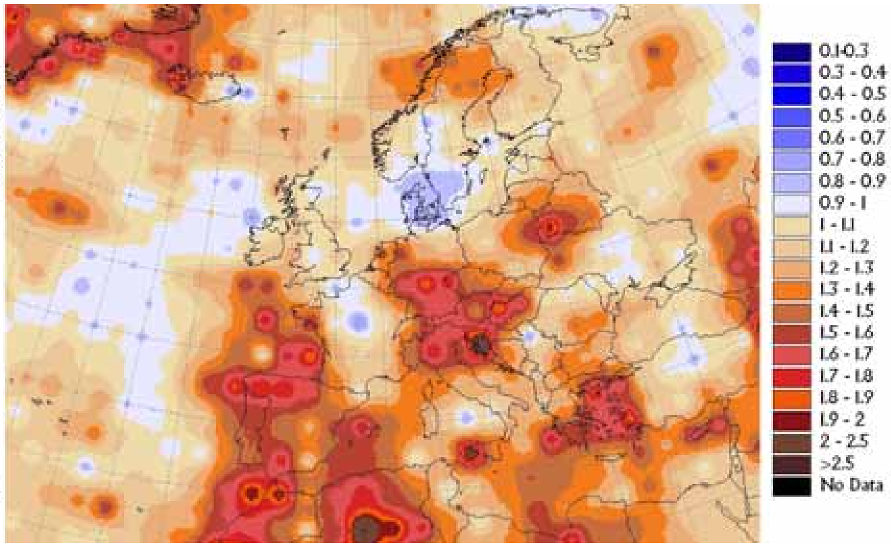

SON

Ratio of standard deviations of the yearly seasonal 90th percentile divergence at 500hPa level

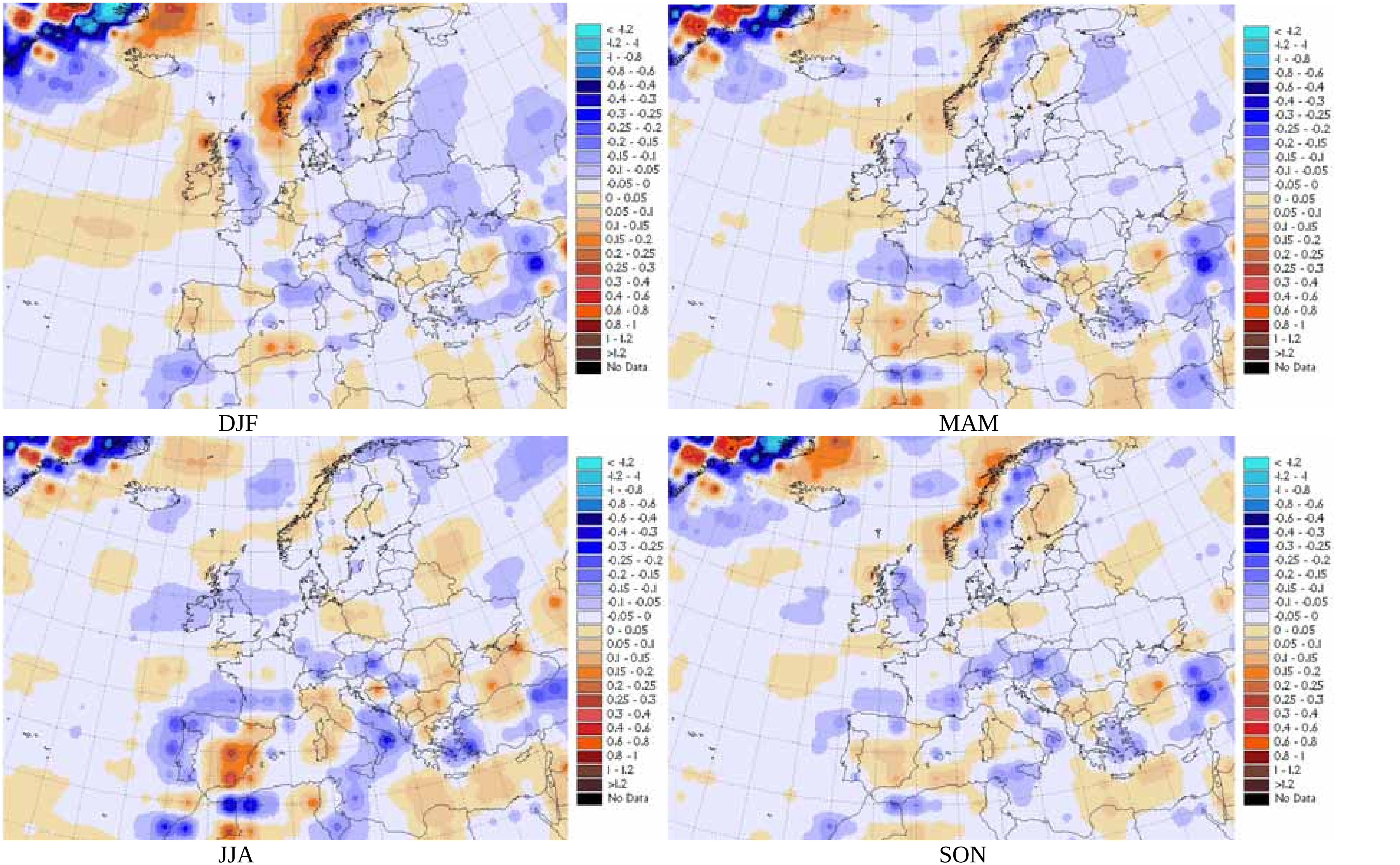

Bias of mean seasonal divergence at 700hPa level (10^{-5}/s)

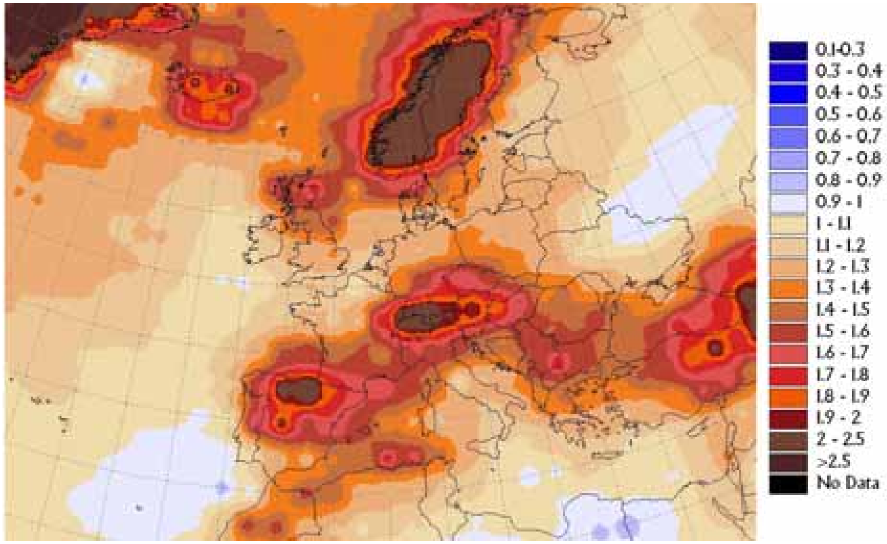

DJF

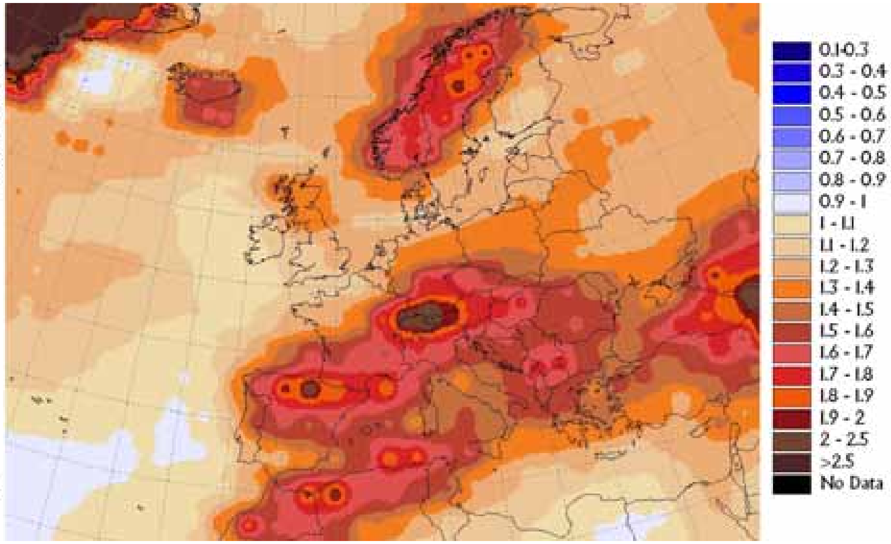

MAM

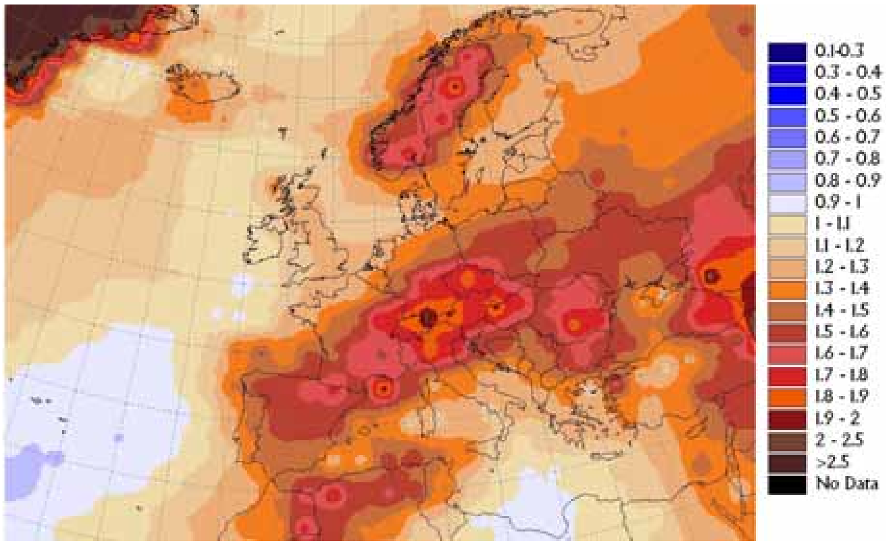

JJA

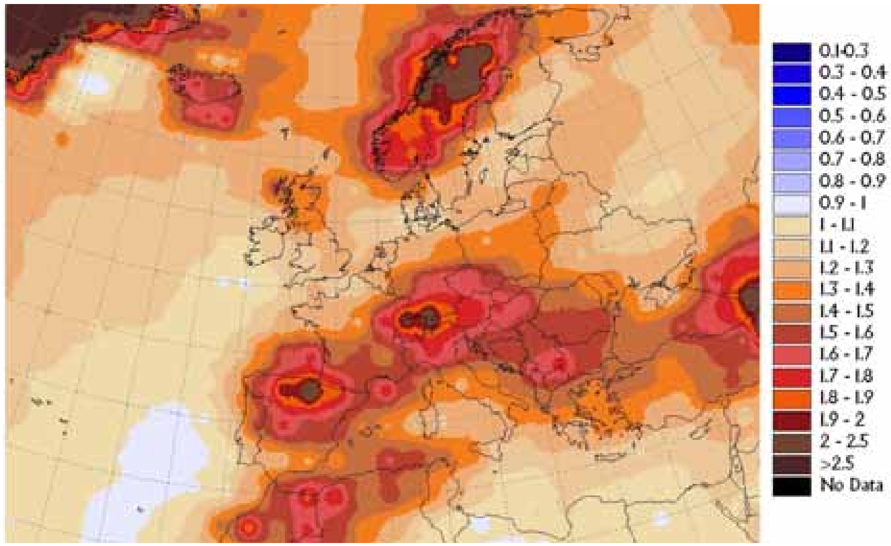

SON

Ratio of standard deviations of daily values of divergence at 700hPa level

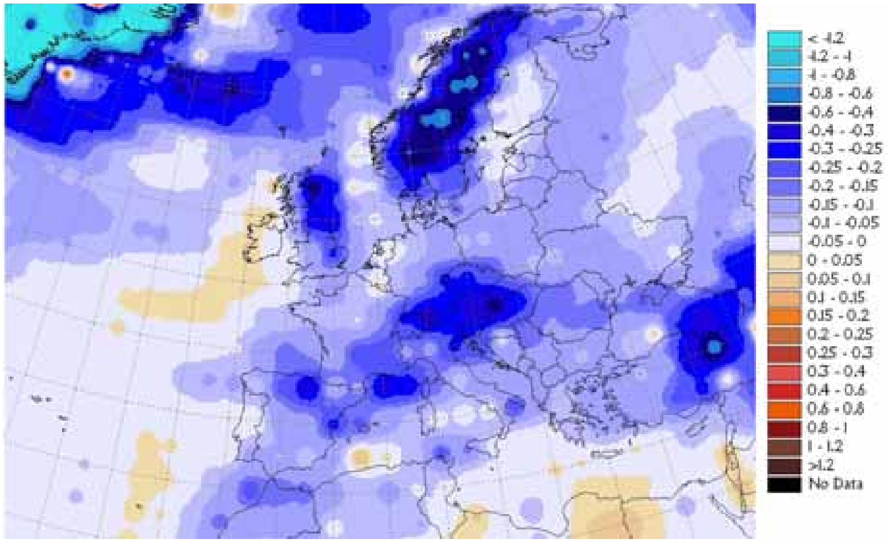

DJF

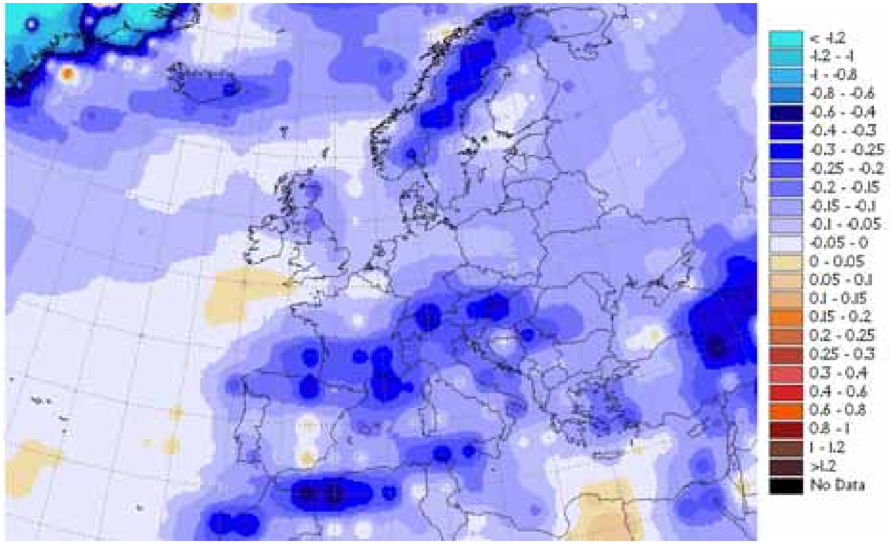

MAM

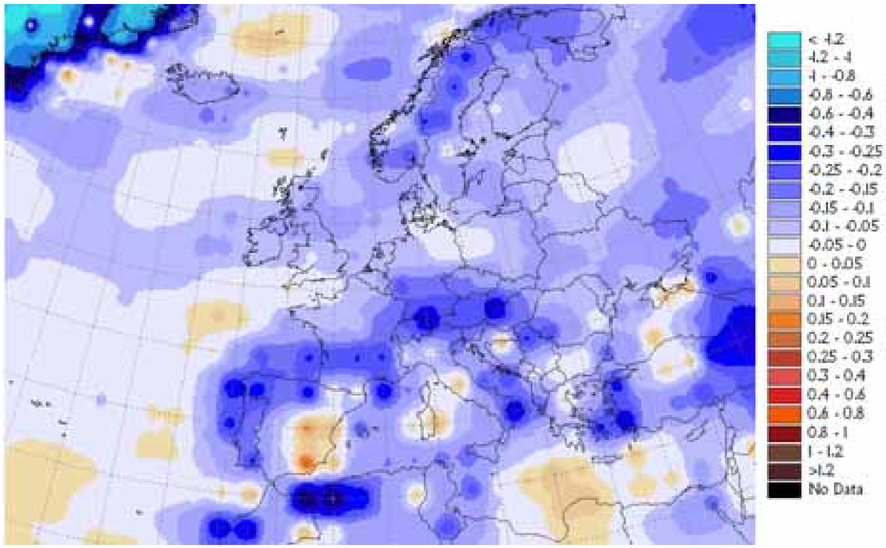

JJA

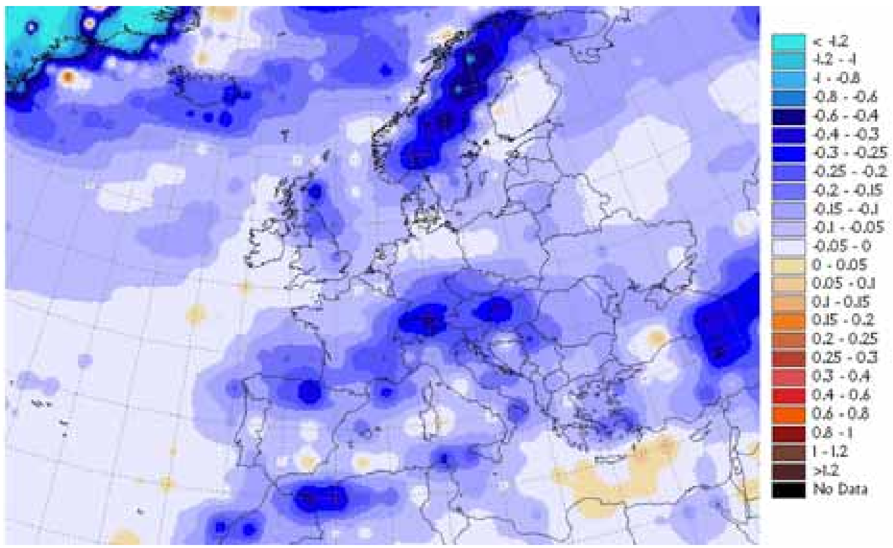

SON

Bias of the average of the yearly 10th percentile seasonal divergence at 700hPa level (10^{-5}/s)

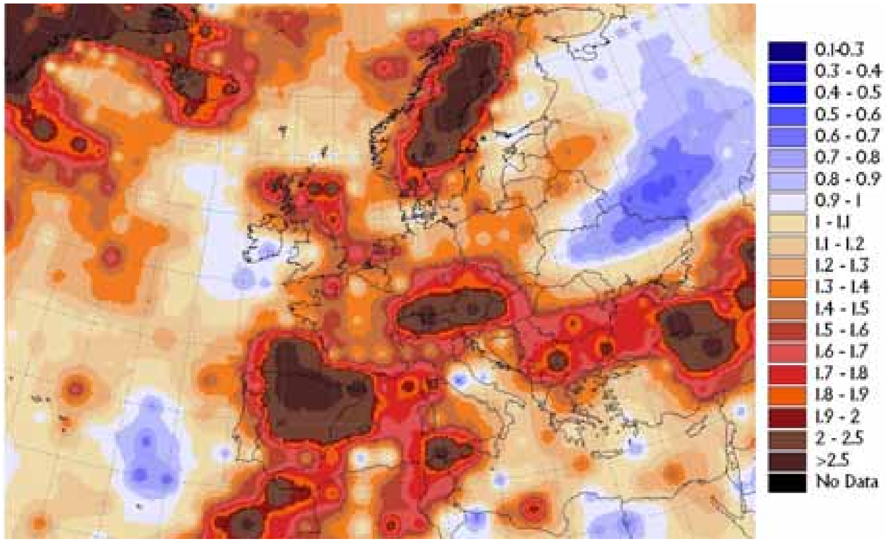

DJF

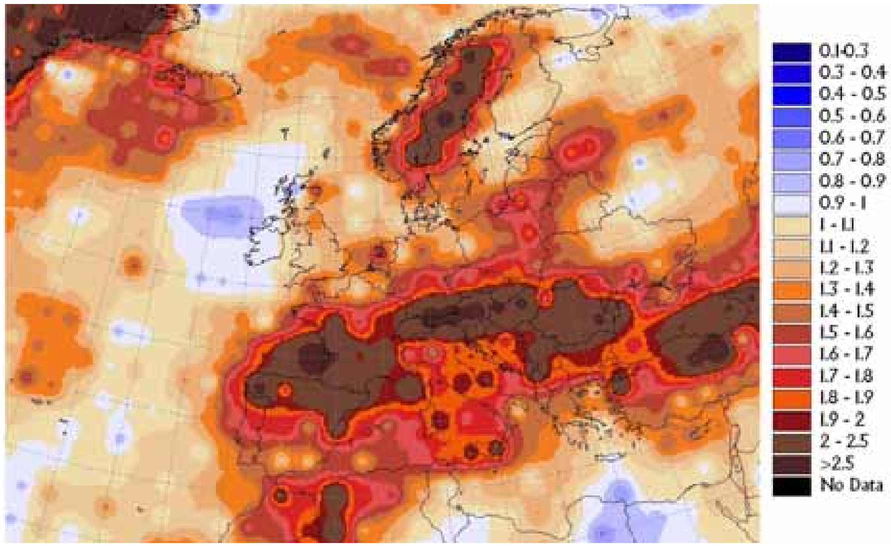

MAM

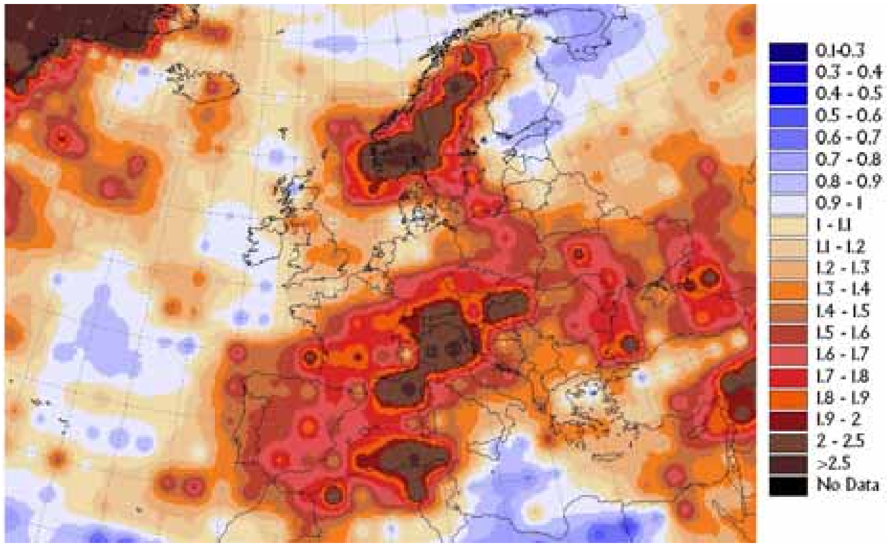

JJA

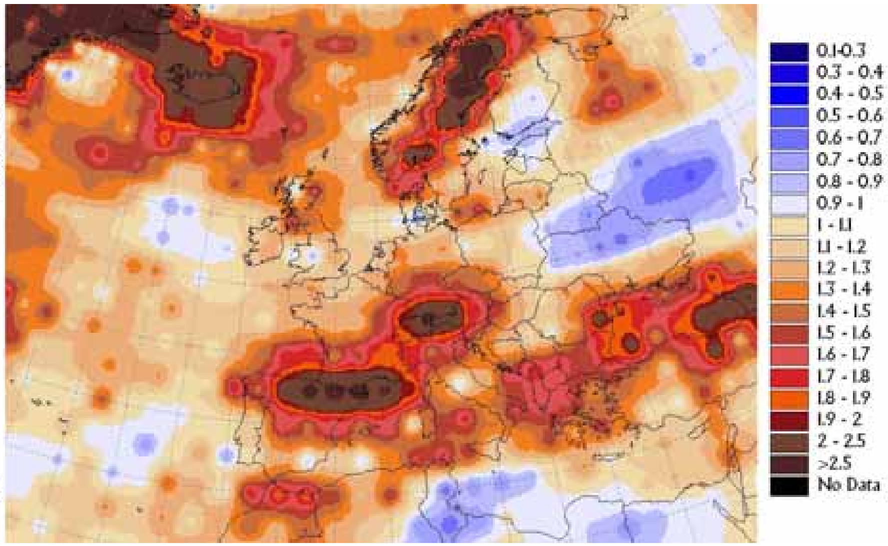

SON

Ratio of standard deviations of the yearly seasonal 10th percentile divergence at 700hPa level

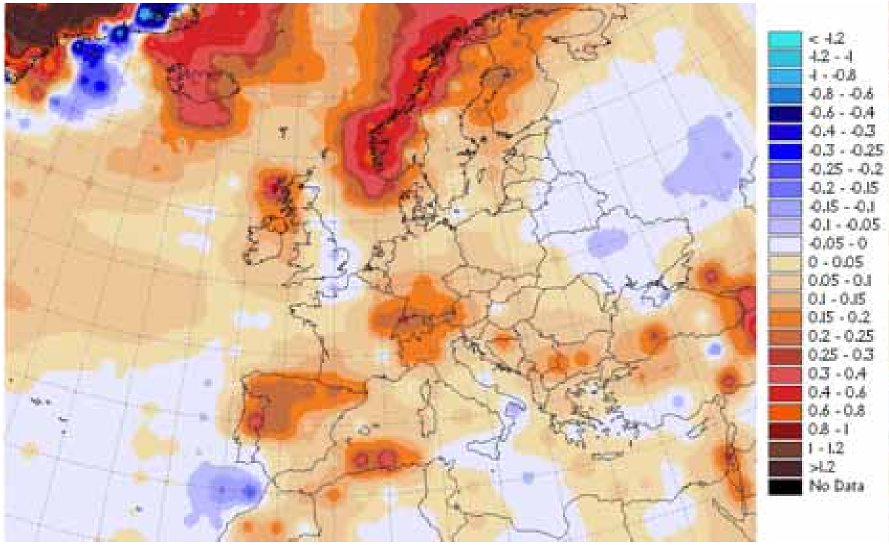

DJF

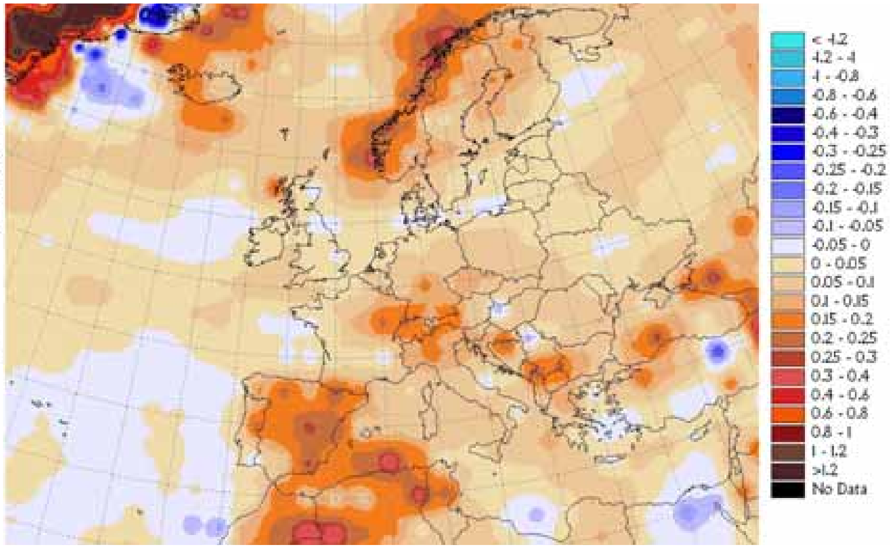

MAM

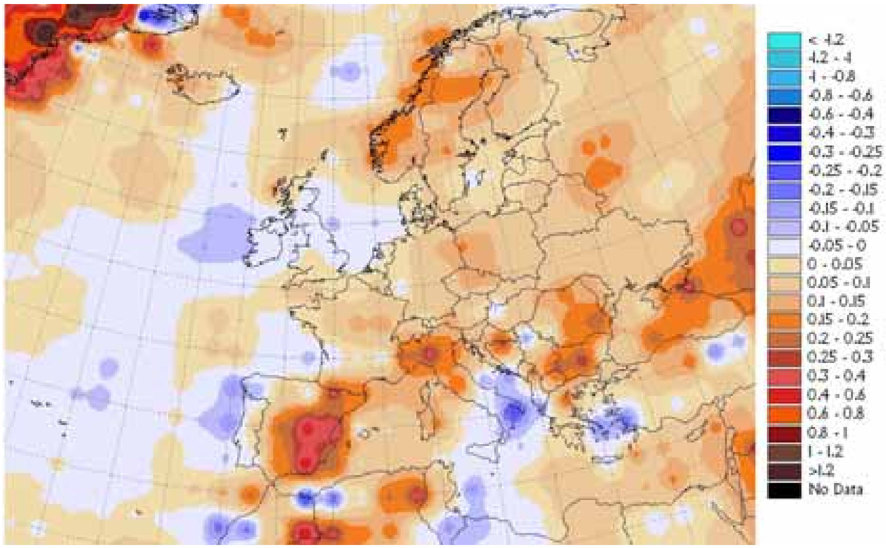

JJA

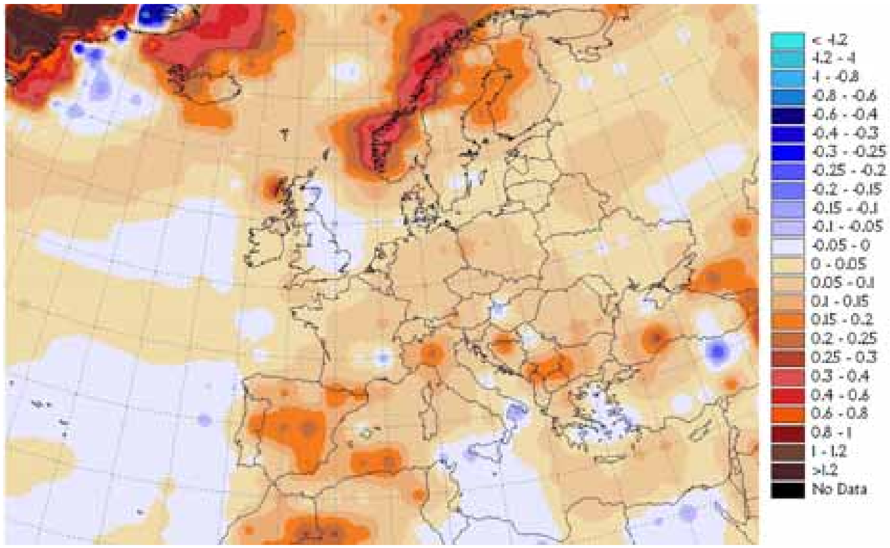

SON

Bias of the average of the yearly 90th percentile seasonal divergence at 700hPa level (10^{-5}/s)

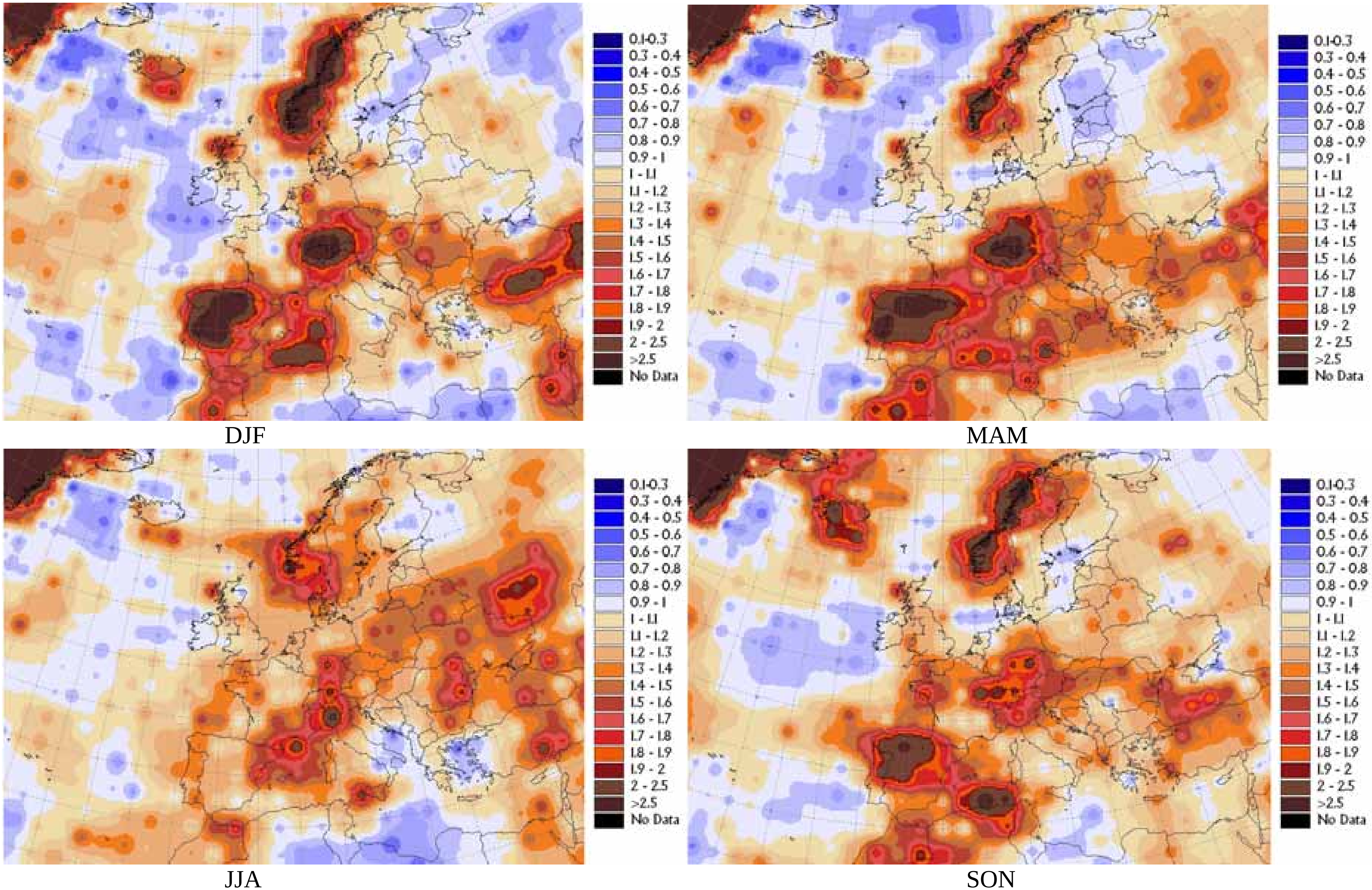

Ratio of standard deviations of the yearly seasonal 90th percentile divergence at 700hPa level

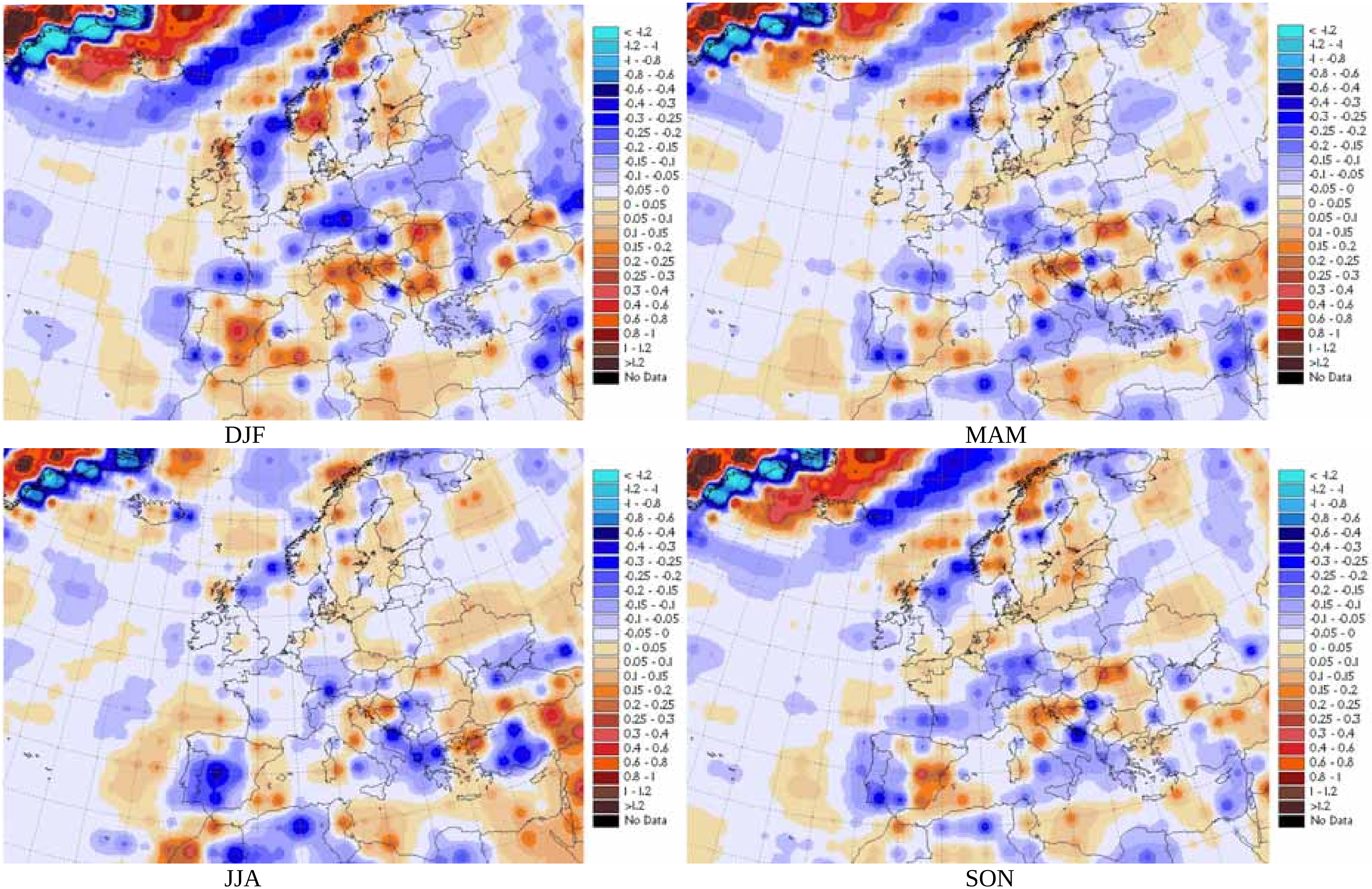

Bias of mean seasonal divergence at 850hPa level (10^{-5}/s)

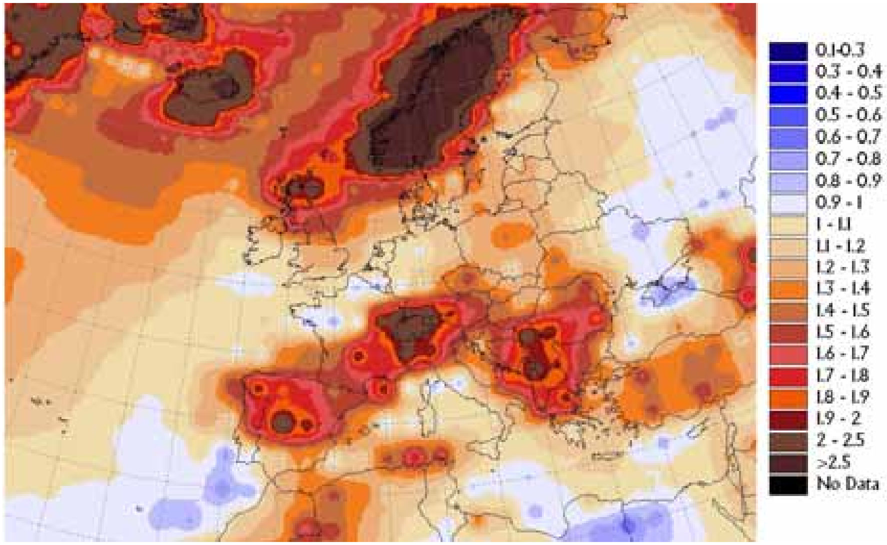

DJF

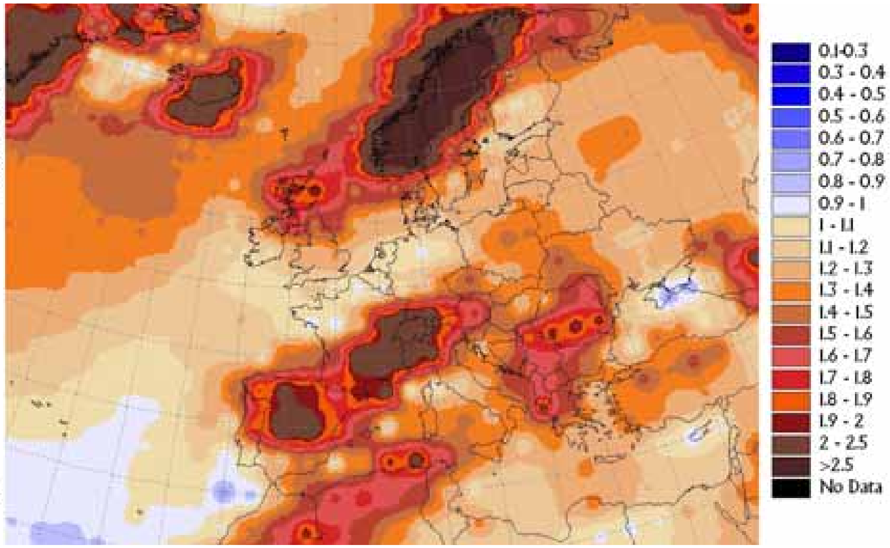

MAM

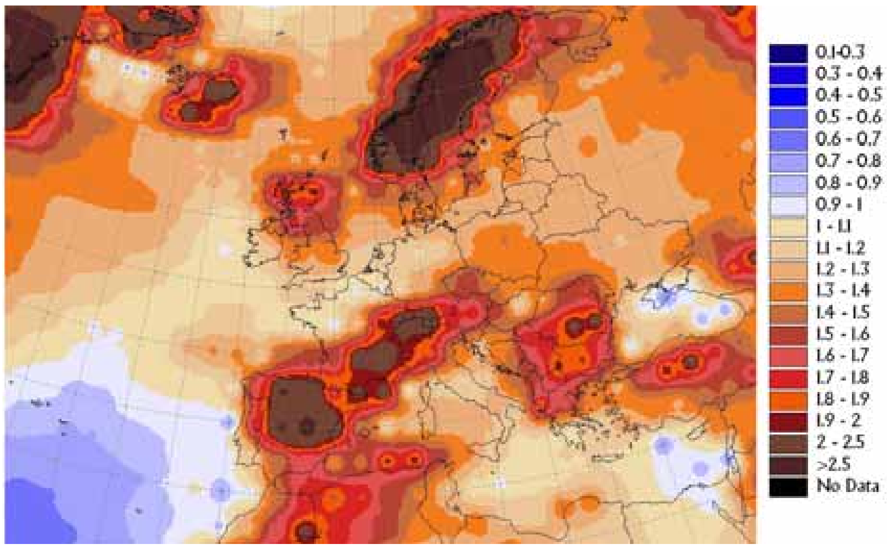

JJA

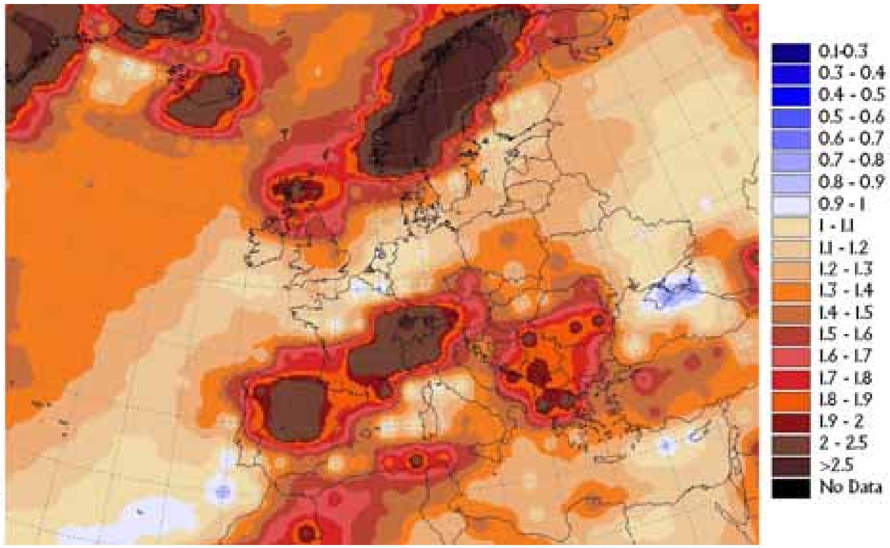

SON

Ratio of standard deviations of daily values of divergence at 850hPa level

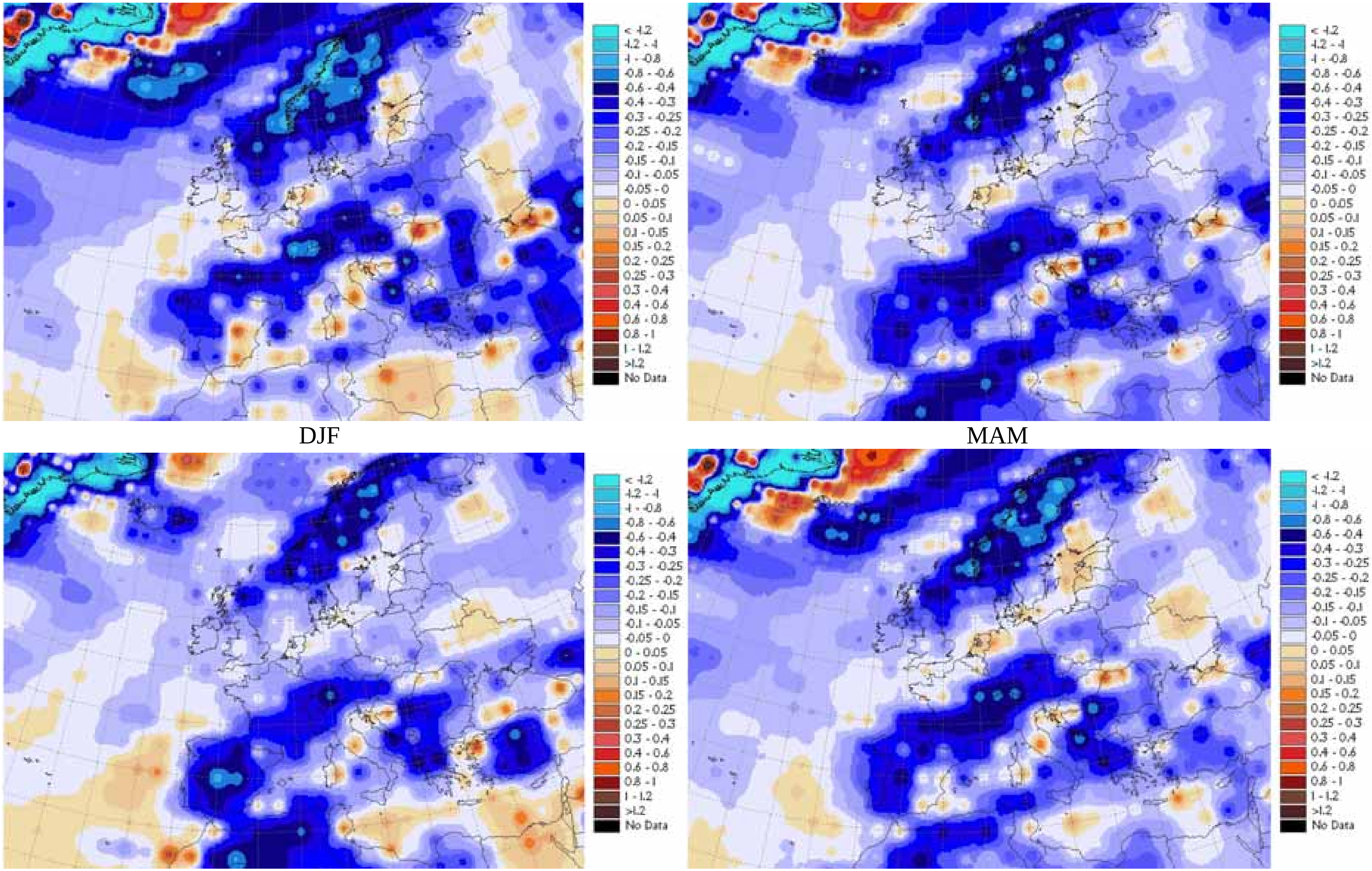

Bias of the average of the yearly 10th percentile seasonal divergence at 850hPa level (10^{-5}/s)

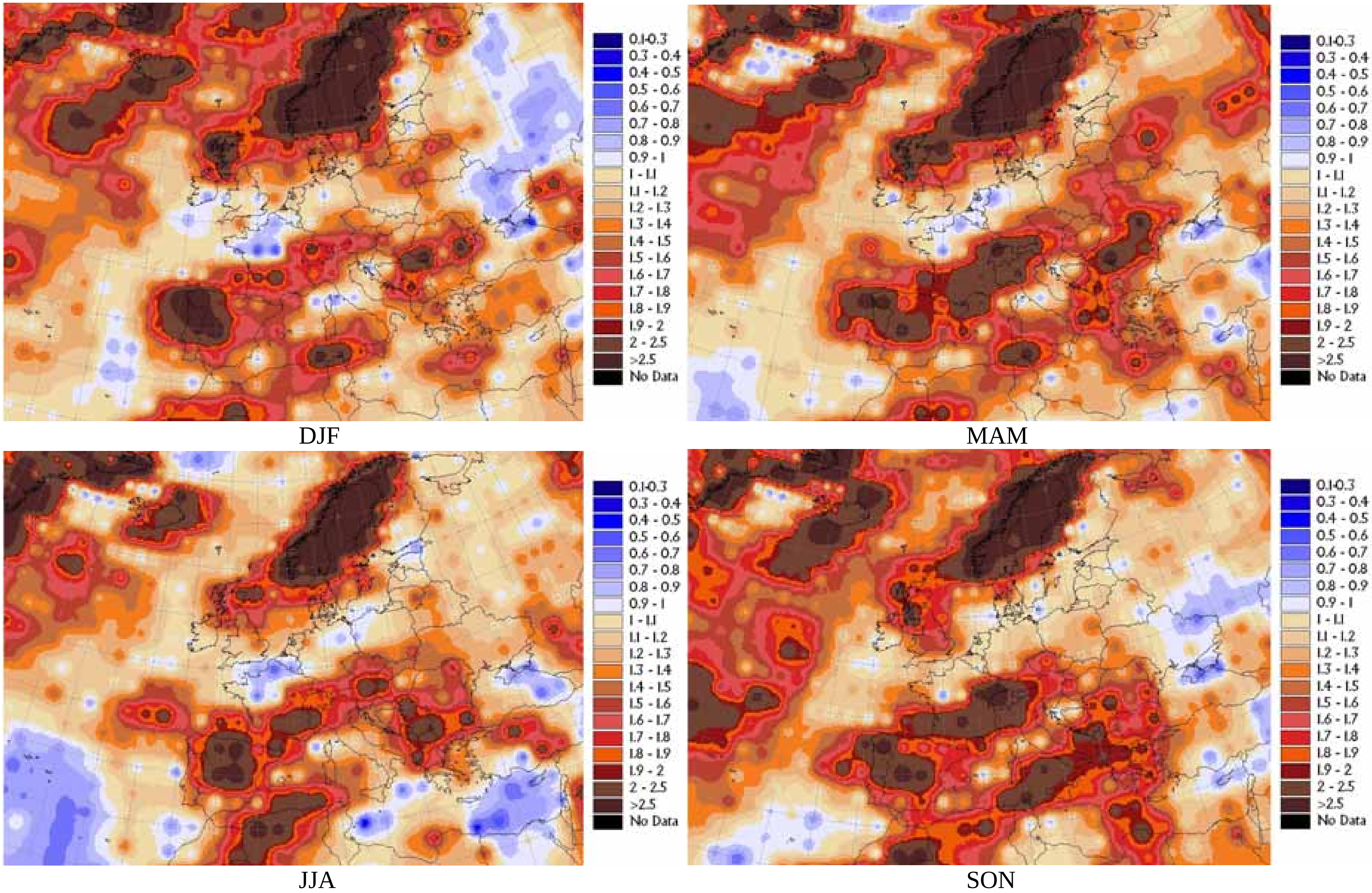

Ratio of standard deviations of the yearly seasonal 10th percentile divergence at 850hPa level

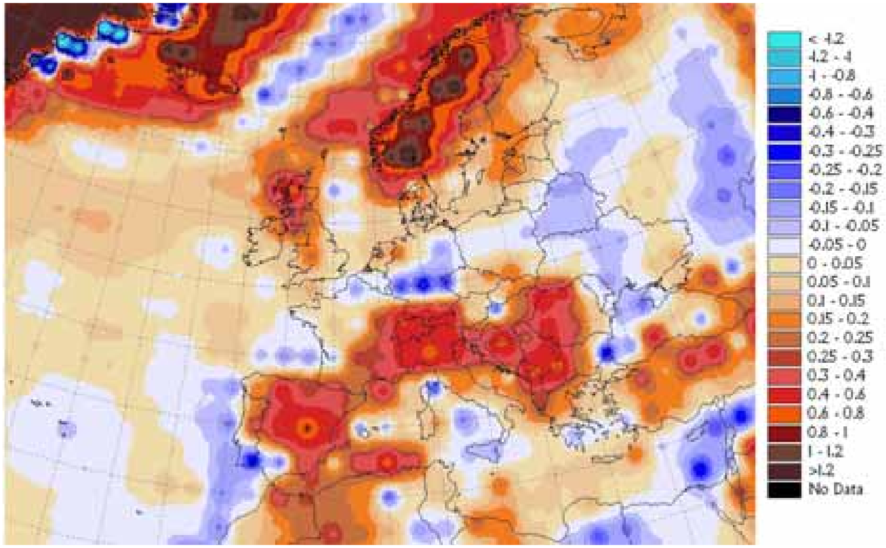

DJF

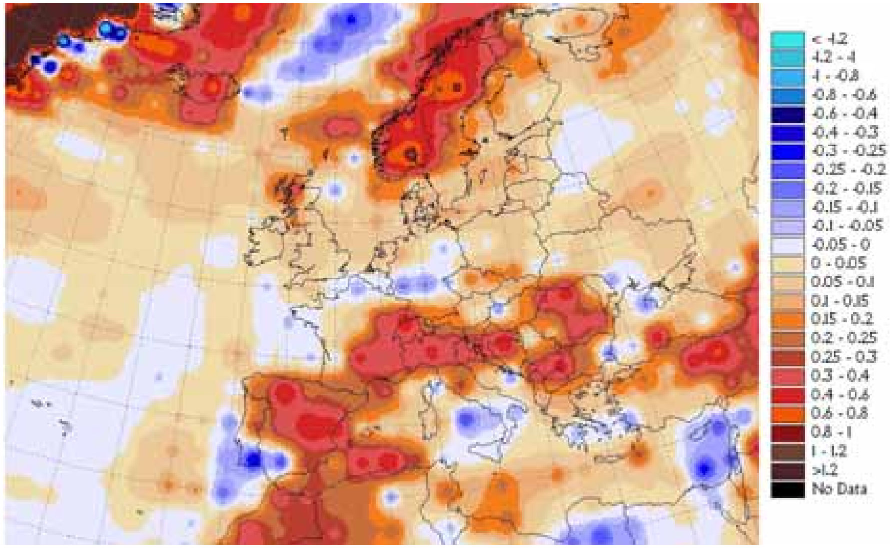

MAM

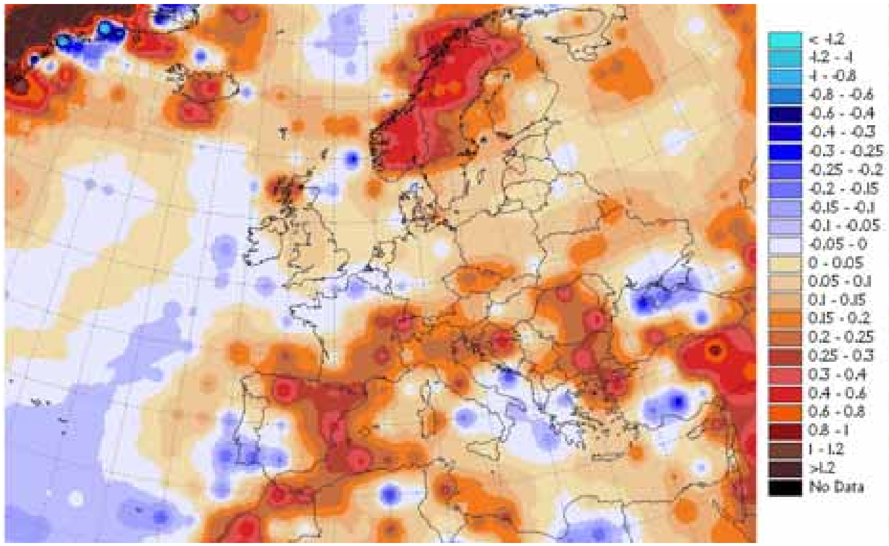

JJA

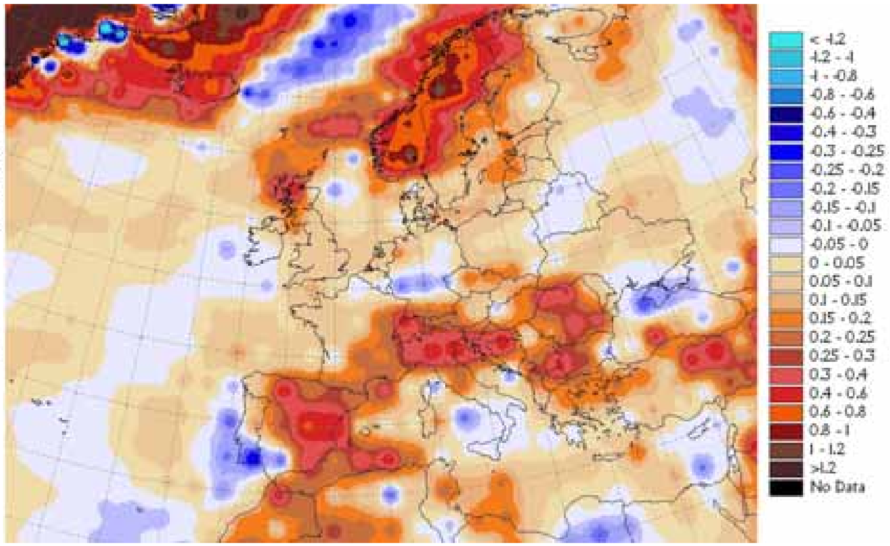

SON

Bias of the average of the yearly 90th percentile seasonal divergence at 850hPa level (10^{-5}/s)

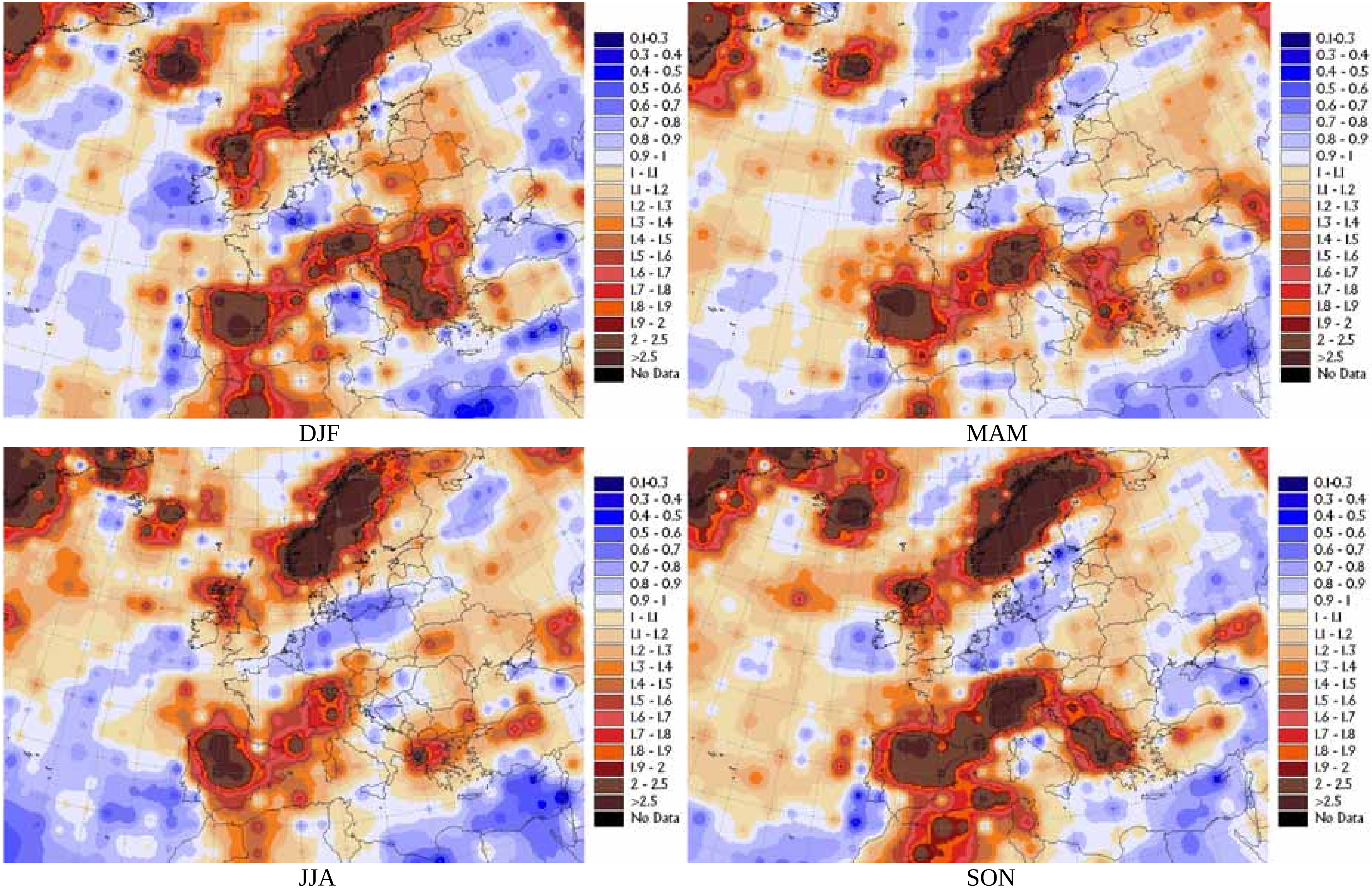

Ratio of standard deviations of the yearly seasonal 90th percentile divergence at 850hPa level